Duality and the approach to scaling in inclusive reactions

Ali, Fouad Hassan

DUALITY AND THE APPROACH TO SCALING IN INCLUSIVE REACTIONS

Thesis submitted to the
University of Durham
by
Fouad Hassan Ali
For the degree of Master of Science
October 1973

Department of Physics,
South Road,
University of Durham
Durham

Acknowledgements

I wish to express my gratitude to my supervisor Dr. P.D.B. Collins for his guidance, encouragement and help.

I also wish to thank Calouste Gulbenkian Foundation for the award of a scholarship.

Many thanks to my friends John and Jenny Evans for the help in correcting the manuscript.

CONTENTS

Abstract			i
Chapter I		Duality and the approach to scaling in two body processes.	1
	I.1	Finite Energy Sum Rules (FESR).	1
	I.2	Application of the FESR, the concept of duality, and the Harari-Freund conjecture.	3
	I.3	Duality diagrams.	7
Chapter II		Inclusive Reactions.	14
	II.1	Introduction.	14
	II.2	Kinematics.	15
	II.3	The hypothesis of a limiting fragmentation and scaling.	17
	II.4	The Generalized Optical Theorem.	19
	II.5	Regge analysis of the inclusive spectra.	20
	II.5.1	The Fragmentation Region.	20
	II.5.2	Double Regge limit - Central Region.	24
Chapter III		Duality and approach to scaling in single particle inclusive reactions.	26
	III.1	Exoticity condition in the fragmentat-ion region.	26
	III.2	Exoticity condition in the central region.	32
Chapter IV		Experimental tests of scaling.	35
	IV.1	Scaling and tests of the exoticity criterion in the fragmentation region.	35

Chapter V The approach to scaling, and conclusions. 40

V.1 The approach to scaling. 40

V.2 Conclusions. 45

References

Figure Captions

Abstract

For two-body processes, duality constraints supplemented by the absence of exotic resonances sucessfully predicted several features of hadronic dynamices. One of these predictions is the early scaling of the total cross-section for exotic processes.

Müller's analysis of inclusive reactions, relating the inclusive cross-section via the generalized optical theorem to the absorptive part of the n-particle forward elastic amplitude, encouraged many people to extend duality arguments, in an attempt to predict when the secondary contributions (or non-scaling part of the amplitude) would be negligible. It seems that this extension is not straightforward, and several criteria have been proposed. In this thesis we try to test these criteria by comaring them with the available data on inclusive reactions at high energies. A major part of the thesis is devoted to a review material concerning the concept of duality and its development.

We begin our review by proving FESR in the classical manner and briefly discuss their application. We show why the Pomeron has an exceptional nature and this, togther with the belive that all resonances should be fitted into SU(3) multiplets, leads to the Harari-Freund conjecture. We also show how it can be represented by two-particle dual diagrams. We then extend this discussion to multiparticle reactions with emphasis on inclusive reactions. We discuss the dual diagrams, the different criteria for scaling and finally some experimental tests.

CHAPTER I

Duality and approach to scaling in two body processes

I.1. Finite Energy Sum Rules (FESR)

FESR are consistency conditions imposed by analyticity on an amplitude which relates its low energy behaviour to its high energy description. To derive the FESR[1] we consider an invariant amplitude $A(\nu,t)$, for fixed t, such that $A(\nu,t)$ is an analytic function in the ν plane, except for a right hand cut along the real axis for $\nu \geq \nu_{th}$, and a left-hand cut symmetric to it. Furthermore we assume that asymptotically the amplitude can be represented by Regge terms[2],

$$A(\nu,t) \xrightarrow[\nu \to \infty]{} \sum_i G_i(t) \frac{-i\pi\alpha_i(t)}{2\sin\pi\alpha_i(t)} + s_i \left(\frac{\nu}{s_o}\right)^{\alpha_i(t)} \qquad \text{(I.1)}$$

where $G_i(t)$ is the residue function of Regge pole, $\alpha_i(t)$ is the trajectory function, s_o is a constant, $s_i = \pm 1$ depending on whether the Regge pole appears in $\pm$ signature partial wave amplitude.

Now consider a countour C as shown in Fig.1.1.

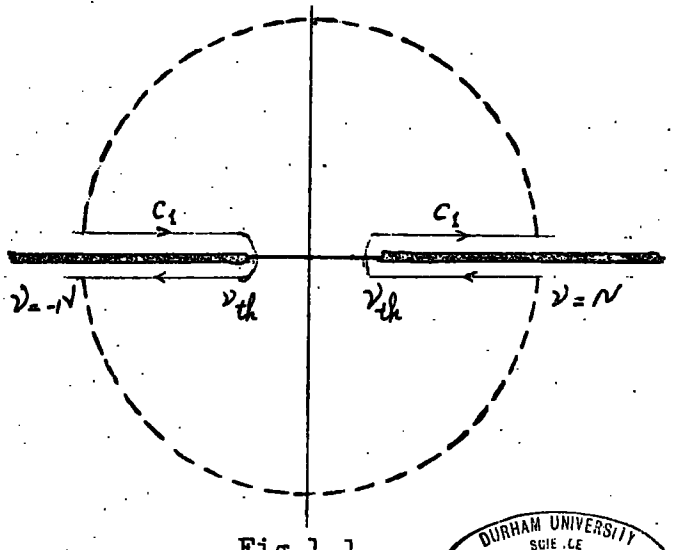

Fig 1.1

By Cauchy's theorem

$$\oint_C A(\nu,t)d\nu = 0 \qquad (I.2)$$

The parts of the contour C along the cuts give

$$\int_{C_1} A(\nu,t)d\nu = 4i\int_{th}^{N} D_\nu(\nu,t)d\nu \qquad (I.3)$$

where the integrand $D_\nu(\nu,t)$ is the discontinuity across the cuts, which is defined by

$$D_\nu(\nu,t) = \frac{1}{2i}\left\{A(\nu+i\epsilon) - A(\nu-i\epsilon)\right\} \qquad (I.4)$$

Assuming that $|\nu| = N$ is high enough such that the asymptotic limit has been reached, replace $A(\nu,t)$ along the two semicircles by its Regge expansion, (I.1). We then deform the contour depending on the different values of $\alpha_i(t)$. For $\alpha_i(t) > 1$ we replace the upper semicircle by a straight line from $\nu = -N-i$ to $\nu = N-i$. This gives

$$-4i\sum_i \int_0^N D_\nu(\nu,t)_{Regge}\, d\nu = -4i\sum_i G_i(t)s_0 \frac{(N/s_0)^{\alpha_i(t)} + s_i}{2\sin\pi\alpha_i(t)}(\nu/s_0)^{\alpha_i(t)} \qquad (I.5)$$

where the discontinuity of the Regge pole terms is

$$D_\nu(\nu,t)_{Regge} = \sum_i G_i(t)(\nu/s_0)^{\alpha_i(t)} \qquad (I.6)$$

For $\alpha < -1$ we expand the semicircle to infinity. Then the contribution of the semicircle will be zero, and the integral along the cut from $\pm N$ to $\pm\infty$ gives the same result as (I.4). Finally for $\alpha_i(t) = -1$ one evaluate the semicircle directly, and obtains a result which is the limit of the cases $\alpha \gtrless -1$.

Putting (1.3) and (1.5) in (1.2) we get

$$\int_{\nu_t}^{N} d\nu D_\nu(\nu,t) = \sum G_i(t) s_o \frac{(N/s_o)^{\alpha_i(t)+1}}{\alpha_i(t)+1} \qquad (I.7)$$

This is the zero moment FESR. For the spin-zero two-particle process, $A(\nu,t)$ represents the scattering amplitude, where ν is our energy variable for a fixed t.

In the physical region we assume that the amplitude is a real analytic function:

$$A^*(\nu,t) = A(\nu^*,t) \qquad (I.8)$$

Then the discontinuity $D_\nu(\nu,t)$ is equal to the imaginary part of the amplitude $ImA(\nu,t)$, and the FESR give an explicit relation between the $ImA(\nu,t)$ at low energies ($\angle N$), and the Regge pole terms at high energies.

One can generalize (1.7) and write higher moment FESR

$$\int_{\nu_t}^{N} (\nu/s_o)^n D_\nu(\nu,t) d\nu = \sum_i G_i(t) s_o \frac{(N/s_o)^{\alpha_i(t)+n+1}}{\alpha_i(t)+n+1} \qquad (I.9)$$

1.2. Application of the FESR, the concept of duality, and the Harari- Freund conjecture.

FESR have a wide range of application. For example, they have been used[3] to determine the parameters of the Regge trajectories.

In fact the trajectory function can be predicted from higher moment FESR using the results

$$\frac{S_m}{S_n} = \frac{\alpha+n+1}{\alpha+m+1} \qquad (I.10)$$

where

$$S_n = \frac{1}{N^{n+1}} \int^{N} \nu^n \mathrm{Im}A^{(-)}(\nu,t)d\nu = \frac{G_A(t)N^{\alpha(t)}}{\alpha_n(t)+n+1} \qquad (I.11)$$

However, our main interest in FESR is in connection with the hypothesis of resonance saturation. At low energy it is useful to represent the amplitude in terms of the s-channel partial waves($s=(P_1+P_2)^2$, where P_1 and P_2 are the four momenta of the incoming particles in the s-channel. The relation between s and the variable ν is given by $\nu = \frac{s-u}{2}$, where $u=(P_1-P_4)^2$). This has the advantage that at low energy the number of the partial waves which give an important contribution is limited, and that often each partial wave can be represented as a sum of resonance poles. If we assume resonance dominance, in other words that at low energy the amplitude is described by resonance contribution only, then one can speak of a duality between the direct channel resonances and the t-channel Regge trajectories. This is a powerful assumption connecting the particles in the two different channnels.In applying FESR to πN-charge exchange (see Fig 1.2) using low energy resonance dominance and high energy Regge dominance, good correlations have been found between the N^* and the ρ Regge trajectory.

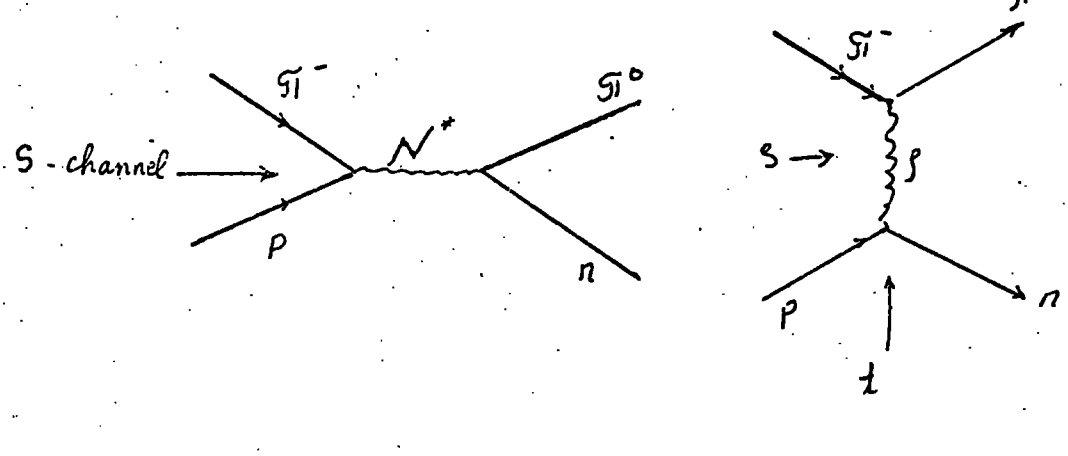

Fig 1.2

However, the concept of resonance dominance can be used only for the imaginary part of the amplitude. If a certain scattering amplitude can be explained by a sum of direct-channel resonances, we approximate its imaginary part at a given energy by the contributions of the resonances in the neighbourhood of that energy. The real part of the amplitude at the same energy will not be described in terms of the nearby resonances. The influence of a resonance on the real part is spread over a wide energy range and in fact, the real part vanishes at the resonance energy.

As far as is known there are no exotic resonances, i.e. all the resonances can be fitted into SU(3) multiplets, which have the internal quantum numbers $(Q, I, I_3, ----)$ given by the quark model, in which mesons are built up from quark-antiquark combinations, and baryons from three quarks qqq.

We know that at high energy and small t, all the elastic processes are controlled by the Pomeranchukon. Applying resonance saturation to exotic processes like pp, K^+p, K^+n, which do not exhibit any direct channel resonances, leads inescapably to the conclusion that the Pomeranchukon is outside the resonances saturation scheme. Indeed it has been shown[4] for $\pi\pi$- elastic scattering, that the resonance approximation can produce the properties of ρ and f but not the P.

Harari[5] noted that the σ_{tot}'s for the exotic processes at high energy are approximately constant, while for processes like $\bar{p}p$, K^-p, and π^+p with a very rich spectrum of s-channel resonances, the σ_{tot}'s vary considerably at high energies.

This lead him to suggest the following conjectures.

1) The low energy background is responsible for building up the Pomeranchukon contributions.

2) The ordinary trajectories (Reggeons) are built up by the low energy resonances, and we can write

$$\mathrm{Im}A(s,t) = R + P \qquad (I.12)$$

where R is the contribution of the direct channel resonances which build up the Reggeon via FESR, and P is the contribu-tion of the non-resonant background in the direct channel which builds up the crossed-channel Pomeranchukon contribu-tion.

It is well known that at high energy the σ_{tot}'s are proportional to

$$\sigma_{tot's} \approx \sum_i s^{\alpha_i(0)-1} \qquad (I.13)$$

with $\alpha_p(0) \simeq 1$ and all others $\alpha_i(0) < 1$ (in fact the intercept for all the leading Reggeons trajectories is $\simeq 1/2$ or $< 1/2$). We see as a conequence of the above conjecture, that the σ_{tot}'s for a process which does not exhibit any resonances is constant, while for those processes which have s or u-channel resonances we need to go to much higher energies to be able to neglect the contribution of the secondaries ($\simeq s^{-1/2}$). Moreover we can say that all σ_{tot}'s must decrease to their asymptotic values. But in the exotic processes like pp and K^+p, in the t-channel we can exchange in addition to the Pomeron the ρ , f, ω , and A_2 trajectories. This would be in contradiction to HF-conjecture, unless we suppose that exchange-degeneracy holds between the Reggeons.

In the absence of the exchange forces, i.e. no u-channel discontinuity, the even and odd signature trajectories will be exchange-degenerate. This would mean that the residues and the trajectory functions were identical. Obviously the difference between two such exchange-degenerate trajectory contributions is purely real

$$G(t)\left\{\left(\frac{e^{i\pi\alpha}+\beta}{2\sin\pi\alpha}\right)-\left(\frac{e^{i\pi\alpha}-\beta}{2\sin\pi\alpha}\right)\right\}(\nu/s_0)^{\alpha}=G(t)\frac{(\nu/s)^{\alpha}}{\sin\pi\alpha} \quad (I.14)$$

Thus for the above reactions (pp and K^+p) where f and A_2, ω and ρ, are exchange-degenerate trajectories, only $I\!P$ contributes to the imaginary part of the amplitude.

1.3. Duality diagrams.

The duality requirement which we have described above can be expressed in terms of dual diagrams Fig.1.3,

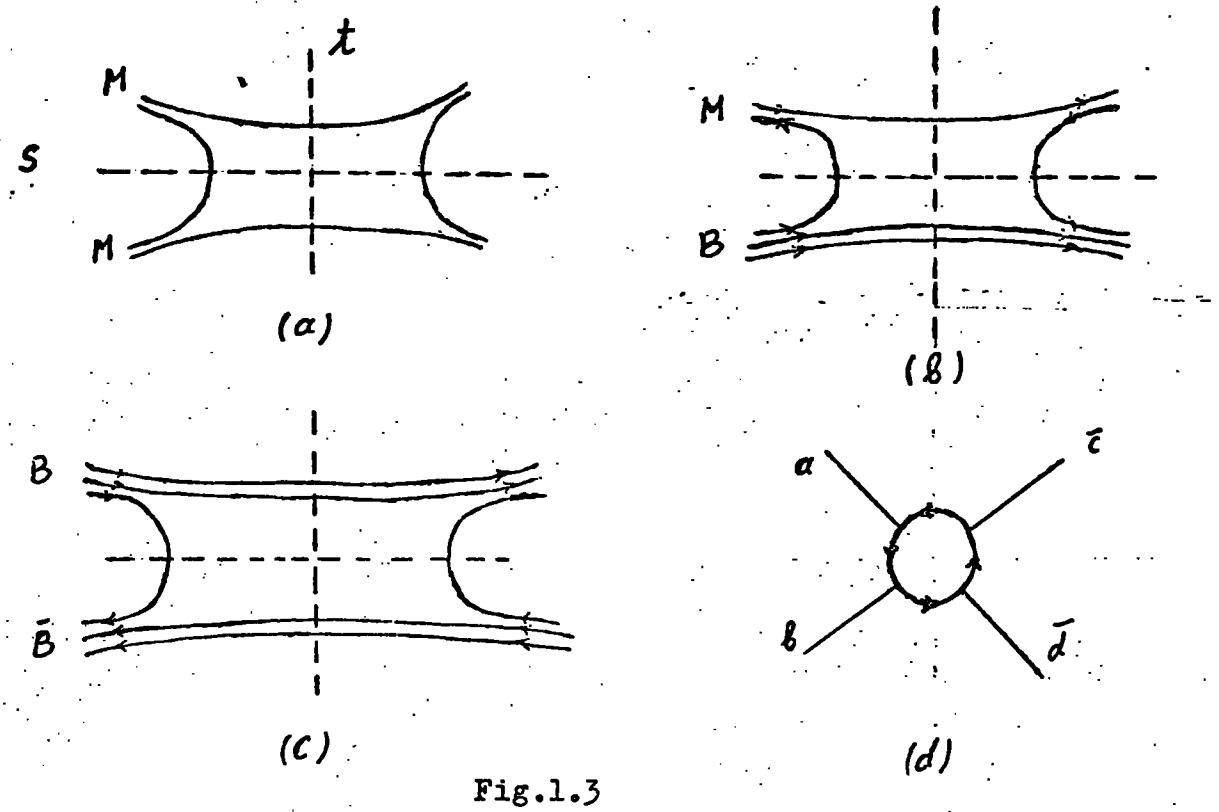

Fig.1.3

where the lines represent quarks. The rules for drawing legal diagrams are :-

1. Every line represents a quark which does not change its identity during the interaction. Therefore every external baryon is represented by three lines in the same direction, and mesons by two lines in opposite directions.

2. The two ends of a single line cannot belong to the same external particle.

In the case of planar diagrams, i.e. those without cross-ing lines we should be able to bisect the diagrams by cutting three lines in the B = 1 channel and only two lines in the B =0 channel.

The diagrams carry information of two types :-

1. The quantum numbers are carried by the quark lines.

2. The topology of the diagrams indicates which channels have the discontinuities. For example the diagrams describing meson-meson and meson-baryon scattering (Fig.1.3,(a)and(b)), have discontinuities in the t and s-channels, but not in the u-channel. Figs.1.3(a) and (b) also demonstrate that there is at least one self-consistent set of amplitudes which satisfies the duality requirements. Here and elsewhere we will use a simple abbreviated form to draw the diagrams, as in Fig.1.3(d), which is equivalent to all other diagrams in Fig.1.3.

In dual perturbative theory[6], we assume that the full scattering amplitude is represented by the sum of all distinct duality diagrams. Therefore within a pole approximation, in addition to Fig.1.3(d) we have to add another two diagrams corresponding to a cyclic inequivalent permutation of the

external particles(Fig.1.4(a)), one of which has a non-vanishing discontinuity in the s and u-channels, the other in u and t-channels (in the Veneziano[7] model these three diagrams correspond to V(s,t), V(s,u), V(u,t)). In addition to the above diagrams we will consider many other, more complicated ones.The main task is to classify them according to their quantum numbers and topology, and to find a simple rule to test whether they are consistent with the Harari-Freund hypothesis.

For the diagram (b)in Fig.1.4, the topology indicates that there are no resonances in the s-channel, since there are no quarks exchanged. Imposing the HF hypothesis, we require that the contribution of this diagram to the imaginary part be zero.

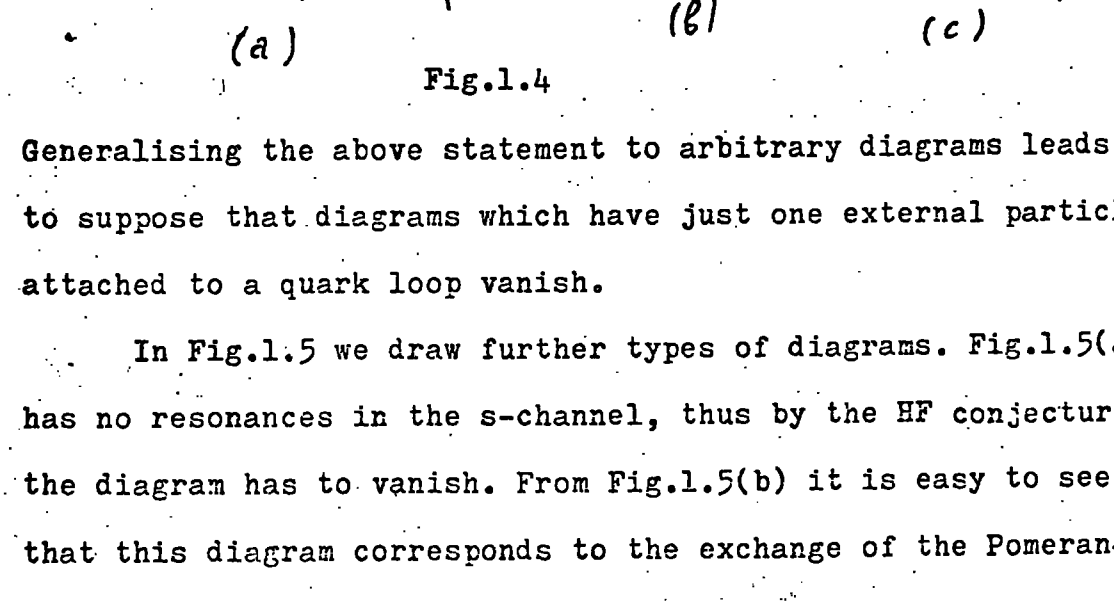

Fig.1.4

Generalising the above statement to arbitrary diagrams leads us to suppose that diagrams which have just one external particle attached to a quark loop vanish.

In Fig.1.5 we draw further types of diagrams. Fig.1.5(a) has no resonances in the s-channel, thus by the HF conjecture, the diagram has to vanish. From Fig.1.5(b) it is easy to see that this diagram corresponds to the exchange of the Pomeran-chukon in the t-channel (the quarks maintain their content,

thus the t-channel has vacuum quantum numbers).

The same can be said about diagrams in Fig.1.5(c) and (d). They have no resonances in t-channel thus they have to vanish.

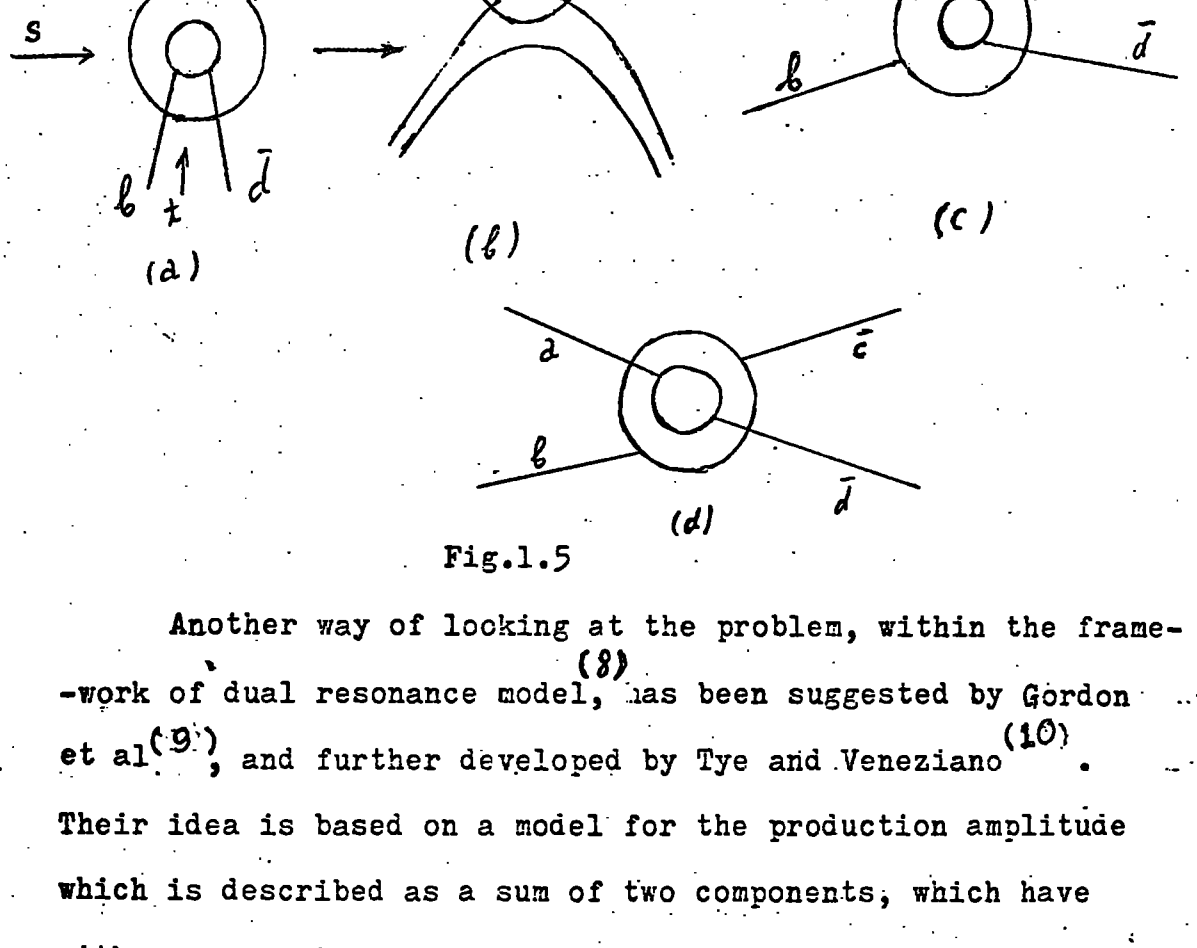

Fig.1.5

Another way of looking at the problem, within the frame-work of dual resonance model,[8] has been suggested by Gordon et al[9], and further developed by Tye and Veneziano[10]. Their idea is based on a model for the production amplitude which is described as a sum of two components, which have either one or two resonances produced in their intermediate states respectively (see Fig.1.6).

Physically the process a+b → anything takes place in three successive steps. The initial state forms a sort of compound state R which decays into the final state, R being either a single resonance or a two-resonance state. In fact the two-resonance state itself is a sum of two terms A_{real}, and A_D, where A_{real} has the same quantum numbers and phase as V(t,u)

in the Veneziano model[11], and A_D , the diffractive component, has vacuum quantum numbers in the t-channel, and is assumed to be purely imaginary.

Thus the production amplitude can be written as a sum of three terms as follows:

$$A(a + b \longrightarrow \text{anything}) \equiv A_{res} + A_{real} + A_D \qquad (I.15)$$

The three components are displayed in Fig.1.6,

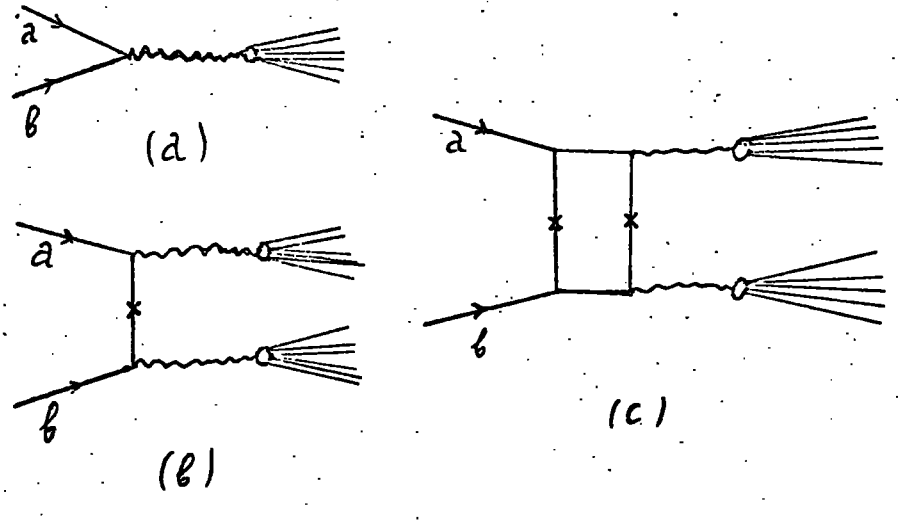

Fig.1.6

where Fig.1.6(a) represents A_{res},(b) represents A_{real}, and (c) represents A_D

It is now easy to see that σ_{tot} is given by (see Fig.1.7)

$$\sigma_{tot} = \sum_{i=1}^{2} \sigma_{ab}^{i} \qquad \sigma_{ab}^{i} > 0 \qquad (I.16)$$

where σ_{ab}^{1} is defined by

$$\sigma_{ab}^{1} = \sigma_{ab}^{res} = \sum A(a + b \longrightarrow R) A^{+}(R \longrightarrow a + b) \qquad (I.17)$$

and σ_{ab}^{2} is equal to

$$\sigma_{ab}^{2} = \sigma_{ab}^{real} + \sigma_{ab}^{D} = \sum_{R_1, R_2} \int \left| A_{real}(a + b \longrightarrow R_1 + R_2) \right|^2 + \left| A_D(a + b \longrightarrow R_1 + R_2) \right|^2 \qquad (I.18)$$

In the above formula σ^1_{ab} is only present if there are resonances in the direct channel. σ^2_{ab} gives the background and has vacuum quantum numbers in the t-channel.

These components of σ_{tot} are shown in Fig.1.7.

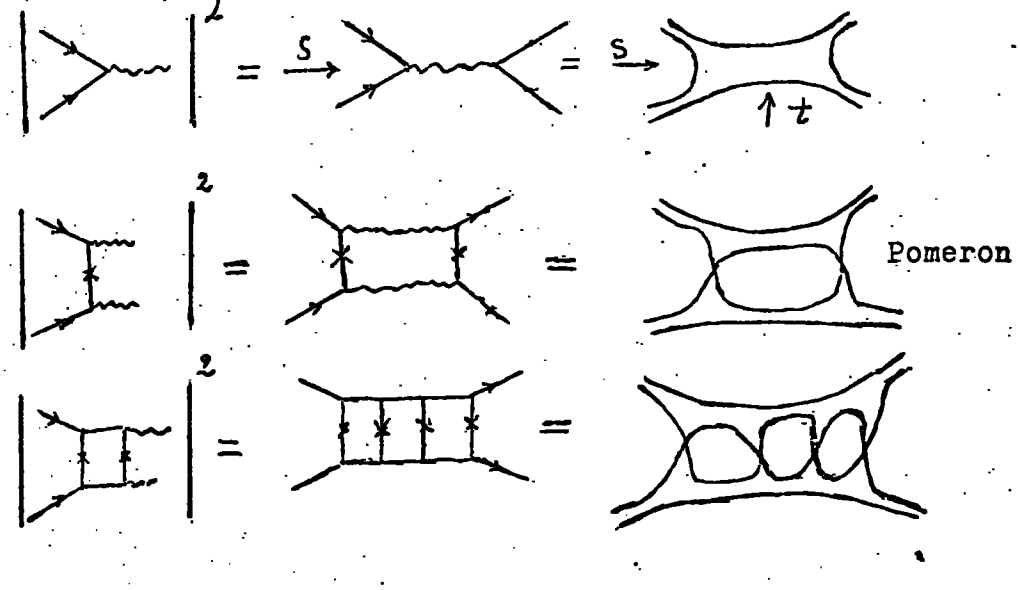

Fig.1.7

Tye and Veneziano call this hypothesis the weak form of the HF-conjecture. By contrast, the strong HF-conjecture is taken to mean the additional assumption, that only the Pomeron is present in σ^2_{tot}. Note that in the previous discussion of the HF-conjecture we implicitly assumed the strong form.

In the above discussion the interfernce terms are always neglected. They may contribute to the real part only, as in the case of A_{real} and A_D, since to the extent that A_D is purely imaginary, this term has a vanishing discontinuity, or they may contribute to some sort of absorpative correction, as in the case of A_{res} and A_D which does not need to be positive definite.

The generalization of dual diagrams to inclusive reactions will be discussed in a later chapter. But we should note here

the fact that they run into difficulties even for two-body scattering. For example, in the case of baryon- antibaryon scattering Fig.1.3(c), we always have the exchange of more quarks than $\bar{q}q$ or qqq in the intermediate state, so we predict that there should be exotic resonances in the direct channel. Another example which could be considered is polarization of in $Kn \longrightarrow \pi^- \Lambda$ at forward angles. The duality diagram Fig.1.8 implies that the amplitude is purely real at high energies. Thus we expect no polarization, but experiments indicate a positive polarization of Λ.

Fig.1.8

CHAPTER II

Inclusive Reactions

II.1 Introduction

In this chapter our concern is to study multiparticle reactions of the form

$$a + b \longrightarrow C_1 + \text{-----} C_m + C_{m+1} \text{------} C_n \qquad (II.1)$$

The most common features, which have been observed experimen-tally in this sort of reaction, are:-

1. Smallness of the transverse momenta P_T.

At high energy the average value of the transverse momenta is of the order of 0.3 GeV/c. It is found to be almost independent of the type of reaction studied, the particle produced, and the incident energy (see Fig.2.1).

2. Low multiplicity of the particles produced.

The average number of particles produced grows much more slowly than is allowed kinematically. It has been suggest-ed that a logarithmic increase of multiplicity occurs when the energy increases.

$$\langle n \rangle = B + A \log s \qquad (II.2)$$

where $\langle n \rangle$ is the average multiplicity defined by

$$\langle n \rangle = \frac{\sum n \sigma^n}{\sum \sigma^n} = \frac{\sum n \sigma^n}{\sigma_{tot}} \qquad (II.3)$$

B and A are constants, σ^n is the cross section for production of n-particles, (see Fig.2.2) .

3. The particles produced are mainly pions (about 90 % at 20 GeV and 80 % at ISR energies).

4. Leading particle effect.

When one of the particles produced has the same quantum numbers as one of the initial particles, it has been observed that it is often produced with a significant fraction of the available energy (see Fig.2.3) .

Combining (1) and (2) we can see that the longitudinal momentum is growing rapidly with energy.

There are two ways of studying multiparticle reactions, exclusively and inclusively. The first description needs a knowledge of the momentum of all the particles produced, the second description needs a knowledge only of the specific particles concerned. In fact the two descriptions are equivalent in the sense that for a full experiment one needs a complete knowledge of all the exclusive cross-sections, which implies a knowledge of all the inclusive cross-sections and vice-versa.[12]

II.2. Kinematics

In this section we discuss the kinematics of the single particle inclusive reaction. Our main task is to define the proper kinematical variables, which we shall need in the later stages of this chapter.

Consider the process

$$P_a + P_b \longrightarrow P_c + X \qquad (II.4)$$

which is described diagramatically in Fig 2.4

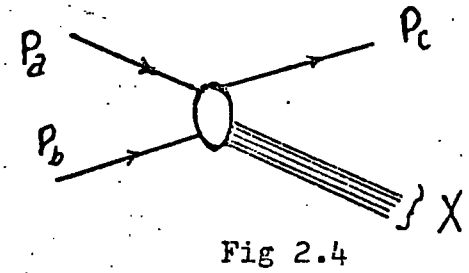

Fig 2.4

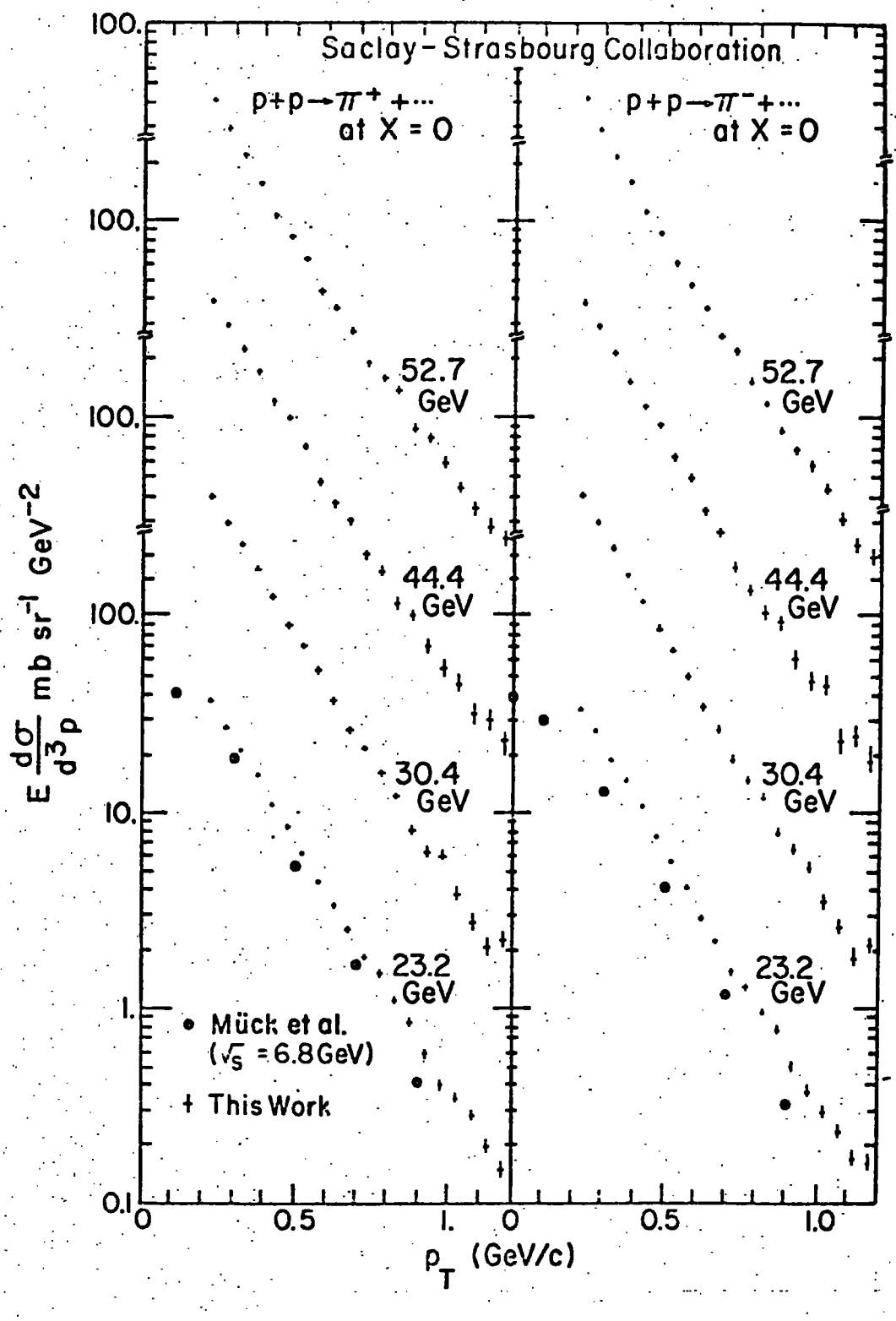
Saclay - Strasbourg Collaboration
p+p→π⁺+···
at X = 0
p+p→π⁻+···
at X = 0
52.7 GeV
44.4 GeV
30.4 GeV
23.2 GeV
Mück et al. (√s = 6.8 GeV)
This Work
E d³σ/d³p mb sr⁻¹ GeV⁻²
p_T (GeV/c)
100.
10.
1.
0.1
0
0.5
1.0

Fig.2.1

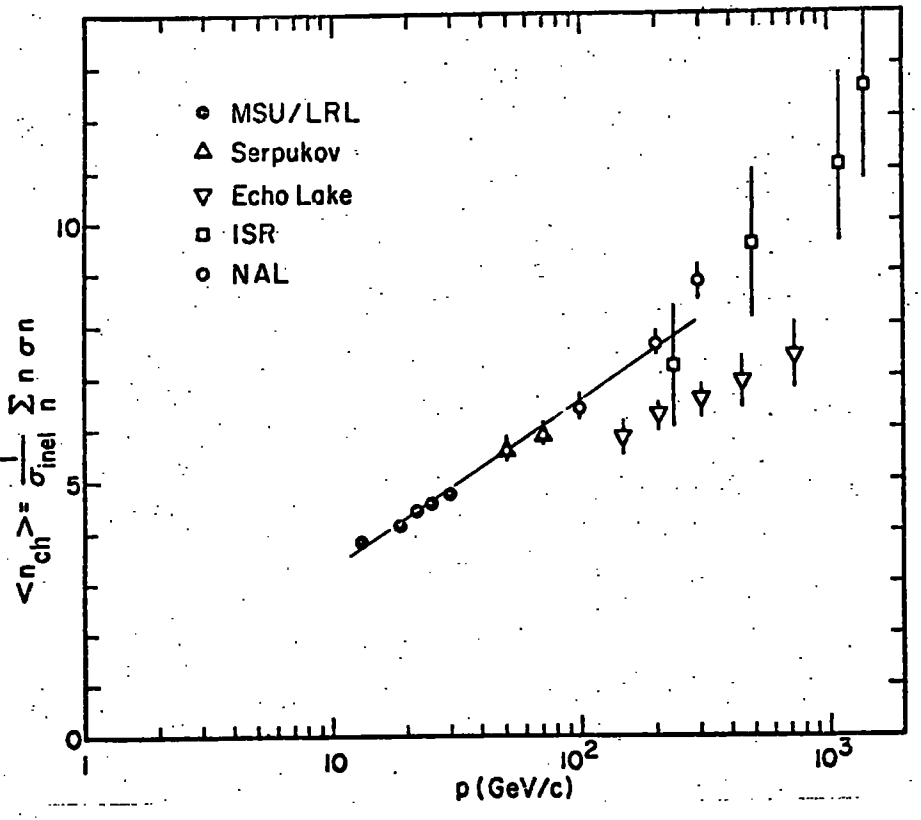
MSU/LRL
Serpukov
Echo Lake
ISR
NAL
$\langle n_{ch} \rangle = \frac{1}{\sigma_{inel}} \sum_n n \sigma_n$
p (GeV/c)

Fig.2.2

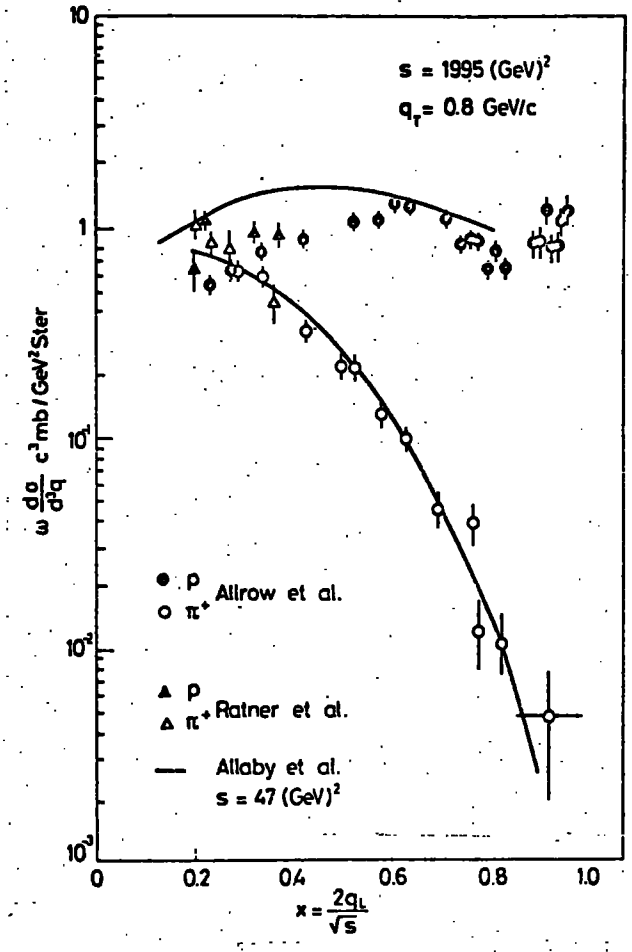
s = 1995 (GeV)²
q_T = 0.8 GeV/c
$\omega \frac{d\sigma}{d^3q}$ c³mb/GeV²Ster
p Allrow et al.
π⁺
p Ratner et al.
π⁺
Allaby et al.
s = 47 (GeV)²
$x = \frac{2q_L}{\sqrt{s}}$

Fig.2.3

where P_a and P_b are the four momenta of the incident and target particles, respectively, P_c is the four momentum of the detected particle, and X represents the other outgoing particles.

In the reaction centre of mass (c.m) system we have

$$\begin{aligned} P_a &= (E_a, 0,0,P_z) \\ P_b &= (E_b, 0,0,-P_z) \\ P_c &= (E_c, P_{cL}, P_{cT}) \end{aligned} \qquad \text{(II.5)}$$

where E_i is the energy of the $i^{\underline{th}}$-particle, P_z is the c.m momentum, P_{cT} and P_{cL} are the transverse and the longitudinal momenta of the particle c.

The rapidity of the particle c in the c.m. system is defined by

$$Y_c = \frac{1}{2} \ln \frac{E_c + P_{cL}}{E_c - P_{cL}} = \sinh^{-1} \frac{P_{cL}}{\mu_c} \qquad \text{(II.6)}$$

where μ_c is the longitudinal mass, and equal to $(m_c^2 + P_{cT}^2)^{1/2}$.

The relation between the Mandelstam invariants and the rapidity are given by

$$s \equiv (P_a + P_b)^2 = m_a^2 + m_b^2 + 2m_a m_b \cosh Y_a^{lab} \qquad \text{(II.7)}$$

$$t \equiv (P_a - P_c)^2 = m_a^2 + m_c^2 - 2m_a \mu_c \cosh Y_c^{proj} \qquad \text{(II.8)}$$

$$u \equiv (P_b - P_c)^2 = m_b^2 + m_c^2 - 2m_b \mu_c \cosh Y_c^{lab} \qquad \text{(II.9)}$$

where Y_a^{lab} is the rapidity of the particle a in the lab system (by the lab system we mean the rest system of the target particle b.), Y_c^{proj} is the rapidity of the particle c in the projectile system (the rest system of the beam particle a), and Y_c^{lab} is the rapidity of the c- particle in the lab system.

Another very useful variable is the missing mass M,

defined by

$$M^2 \equiv (P_a + P_b - P_c)^2 = s + m_c^2 - 2s^{1/2}\mu_c \cosh Y_c . \qquad (II.10)$$

Feynman defines a new variable as follows :

$$X_c = \frac{2P_{cL}}{\sqrt{s}} \qquad (II.11)$$

To specify a single particle inclusive reaction one can take any three independent variables from the above set.

The relation between the longitudinal momentum of the particle c in the lab system $q_{c//}$ and the Feynman variable X is given by the Lorentz transformation

$$q_{c//} = \frac{1}{2}\sqrt{s}\left\{\sinh u \left[X^2 + 4\frac{\mu_c^2}{s}\right]^{1/2} + X \cosh u\right\} \qquad (II.12)$$

where $\sinh u = P_z/m_b$

Dividing the missing mass M^2 by s, asymptotically we obtain

$$\frac{M^2}{s} = 1 + \frac{m_c^2}{s} - \left(X^2 + \frac{4\mu_c^2}{s} \right)^{1/2} \simeq 1 - |X| \qquad (II.13)$$

where we have replaced $\cosh Y_c$ by

$$\cosh Y_c = \left(\frac{X_c^2 s}{2\mu_c} + 1\right)^{1/2} \qquad (II.14)$$

and finally we write the variable t in terms of X and P_{cT}

$$t = m_a^2 + m_c^2 - m_a\mu_c\left(\frac{m_a X}{c} + \frac{\mu_c}{m_a X}\right)$$

$$\simeq - P_{cT}^2/X + m_a^2(1 - X) + m_c^2(1 - X) \qquad (II.15)$$

II.3 The hypothesis of a limiting fragmentation and scaling

It is covenient to represent the unpolarized inclusive cross-section by the invariant function $f_1^{c,ab}$ called the single particle distribution or spectral function and defined by

$$E_c \frac{d^3}{dP_c^3} \equiv f_1^{c,ab}(P_c, s) \qquad (II.16)$$

Multiparticle inclusive spectra can also be defined as

$$\prod_{i=1}^{n} E_i \frac{d\sigma^{in}}{dP_1^3 \cdots dP_n^3} \equiv f_{ab}^{c_1 \cdots c_n}(s, P_{c_1}, \cdots, P_{c_n}) \qquad (II.17)$$

Another useful function is the density function which is defined by

$$\rho_{ab}^{c_1 \cdots c_n} = \frac{1}{\sigma_{ab}} f_{ab}^{c_1 \cdots c_n} \qquad (II.18)$$

The limiting fragmentation hypothesis (Benceke, Chow, Yang and Yen[13]) states that in the lab system (projectile system) some of the outgoing particles with small longitudinal momenta (BCYY describe them as fragments of the target (projectile)) approach a limiting distribution as $s \to \infty$. In terms of spectral function this hypothesis reads

$$\lim f_1^{c,ab}(q_{c\parallel}, q_{cT}, s) = f_1^{c,ab}(q_{c\parallel}, q_{cT}) \qquad (II.19)$$

provided $q_{c\parallel}$ is held fixed.

The scaling hypothesis which has been proposed by Feynman[14] states that if we consider the spectral function $f_1^{c,ab}$ as a function of the centre of mass variables then we have

$$\lim_{s \to \infty} f_1^{c,ab}(P_{cL}, P_{cT}, s) \simeq f_1^{c,ab}(X, P_{cT}) \qquad (II.20)$$

independent of s.

For $X \gg 4\mu_c^2/s$, the two hypotheses are equivalent. This can be seen from (II.12), since the asymptotic behaviour of $q_{c\parallel}$ for large s, small q_{cT}, and $X \ll 2\mu_c/s^{1/2}$ is given by

$$q_{c\parallel} = \frac{1}{2} m_b X - (\mu_c^2/2Xm_b) \qquad (II.21)$$

We see that fixed X implies fixed $q_{c\parallel}$ in the lab system. It can be shown that for $X \gg 2\mu_c/s^{1/2}$, fixed X implies fixed $q_{c\parallel}$ in the projectile system. However the point X = 0 does not correspond

to any finite momentum in the lab or projectile systems. Feynman makes the further prediction that, near the point $X = 0$, $f^{c,ab}$ is independent of X.

II.4 The Generalized Optical Theorem.

The generalized optical theorem plays, in inclusive reactions, the same role as the ordinary optical theorem does for the total cross-section.

The optical theorem, based on unitarity, says that the cross section for the process a + b ⟶ anything is equal to the imaginary part of the elastic amplitude a + b ⟶ a + b in the forward direction (see Fig.2.5)

$$\sigma_{tot} = \frac{1}{flux} \text{Im } A^{el}_{ab}(s,t = 0) \qquad (II.22)$$

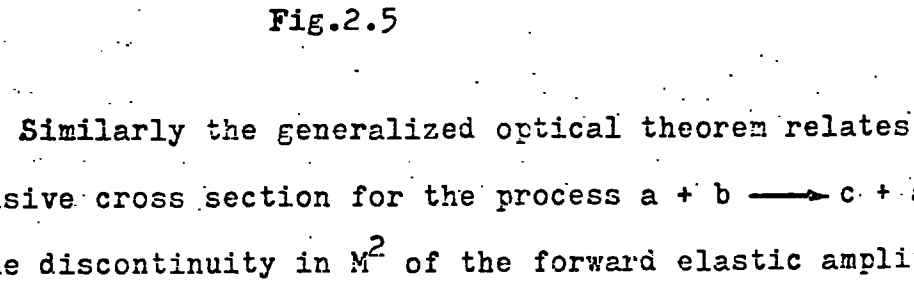

$$\xrightarrow{\text{Unitarity}} \quad \text{Im } A^{el}_{ab}(s,t = 0)$$

Fig.2.5

Similarly the generalized optical theorem relates the inclusive cross section for the process a + b ⟶ c + anything to the discontinuity in M^2 of the forward elastic amplitude of the process

$$a + b + c \longrightarrow a + b + c \qquad (II.23)$$

If one considers the amplitude as a function of s, M^2, and t then the generalized optical theorem can be written as

$$f_1^{c,ab}(s,M^2,t) = \frac{1}{s} \text{Dis}_{M^2}(s,M^2,t) \qquad (II.24)$$

where the $\mathrm{Dis}_{M^2}(s,M^2,t)$ is defined by

$$\mathrm{Dis}_{M^2}(s,M^2,t) = \frac{1}{2i}\Big\{ A(s + i\varepsilon, M^2 + i\varepsilon, t - i\varepsilon) - A(s + i\varepsilon, M^2 - i\varepsilon, t - i\varepsilon)\Big\} \qquad (II.25)$$

This relation is shown pictorially in Fig.2.6

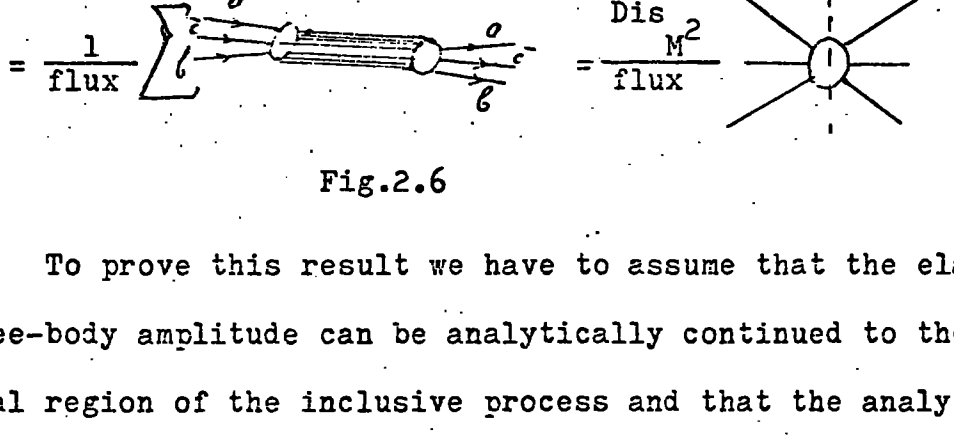

Fig.2.6

To prove this result we have to assume that the elastic three-body amplitude can be analytically continued to the phys-ical region of the inclusive process and that the analytic continuation describes the actual physical situation there.

II.5 Regge analysis of the inclusive spectra.

The importance of the above theorem lies in the fact that in a certain asymptotic limit the forward three-body elastic amplitude can be expanded in terms of Regge singularities. In this way one obtains an asymptotic Regge expansion of the in-clusive spectra. We shall make use of the generalized optical theorem in two different regions, the fragmentation region and the pionization region.

II.5.1 The Fragmentation Region.

In this region one can consider three different limits, the single Regge limit, the normal Regge limit and the triple Regge limit.

Single Regge limit.

Consider the distribution function $f_1^{c,ab}$ as a function of the three independent variables, s, t, M^2/s, where M^2/s is the Toller angle describing the orientation of $b\bar{c}$ with respect to the scattering plane defined by $b\bar{c}$ and a.

In terms of the above variables the single Regge limit is defined by $s \to \infty$, t and M^2/s fixed. It is easy to see that this limit is identical with the fragmentation limit. Indeed from (II.13) we find that fixed M^2/s implies fixed X, and furthermore from (II.15) we see that fixed X and t imply fixed q_{cT}^2, or equivalently fixed m_c^2. Since m_c^2 is fixed then $X^2 \gg 4m_c^2/s$, and we have already indicated that this limit is identical with the fragmentation limit in the lab system for $X \ll 2m_c/s^{1/2}$, and identical with the fragmentation limit in the projectile system for $X \gg 2m_c/s^{1/2}$.

Then the Regge model for the elastic amplitude gives the following asymptotic expansion, as illustrated in Fig.2.7.

$$f(s, M^2/s, t) = \sum \beta_i(M^2/s,t)(M^2)^{\alpha_i(0)-1} \qquad (II.26)$$

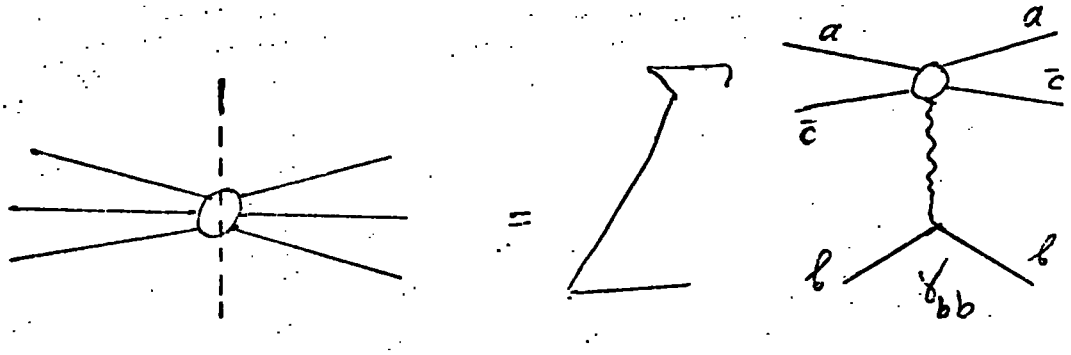

Fig.2.7

To obtain (II.26) we have to assume pole dominance. Assuming the dominance of the Pomeron $\mathbb{P}$ with intercept one ($\alpha_{\mathbb{P}} = 1$), and the meson trajectories ρ, f, ω, and A_2 with intercept one-half ($\alpha_M = 1/2$) one has:

$$f(s,M^2/s,t) \cong \beta_{\mathbb{P}}(M^2/s,t) + \sum \beta_M(M^2/s,t)s^{-1/2} \qquad (II.27)$$

When s is sufficiently large we obtain

$$f(s,M^2/s,t) \cong \beta_{\mathbb{P}}(t,M^2/s) \qquad (II.28)$$

thus the single particle distribution function $f_1^{c,ab}$ becomes independent of energy. This is in fact the limiting fragmentation hypothesis of Yang, or the scaling hypothesis of Feynman, since both hypotheses are equivalent in the fragmentation region.

If the Pomeron factorises then one has

$$f_1^{c,ab} \cong \gamma_{bb}^{\mathbb{P}} \beta_{a\bar{c},a\bar{c}}^{\mathbb{P}}(M^2/s,t) \qquad (II.29)$$

where the dependence on the target particle b is contained in the factor $\gamma_{bb}^{\mathbb{P}}$, while $\beta_{a\bar{c},a\bar{c}}^{\mathbb{P}}(M^2/s,t)$ depends on the variables describing the cluster $a\bar{c}$.

Now suppose we replace the cluster $a\bar{c}$ by a genuine particle say a, i.e. we consider the ba total cross-section, then asymptotically one has

$$\sigma_{tot}^{ab} = \gamma_{bb}^{\mathbb{P}} \gamma_{aa}^{\mathbb{P}} \qquad (II.30)$$

Dividing $f_1^{c,ab}$ by σ_{tot}^{ab}, one finds that the density function in the projectile system is independent of the nature of the target.

$$\rho_{ab}^{c} = \frac{f^{c,ab}}{\sigma_{tot}^{ab}} \beta_{a\bar{c},a\bar{c}}^{\mathbb{P}} / \gamma_{aa}^{\mathbb{P}} \qquad (II.31)$$

Normal and Triple Regge limit.

In the fragmentation region there are two other limits to be considered, the normal and the triple Regge limits

(see Fig.2.8).

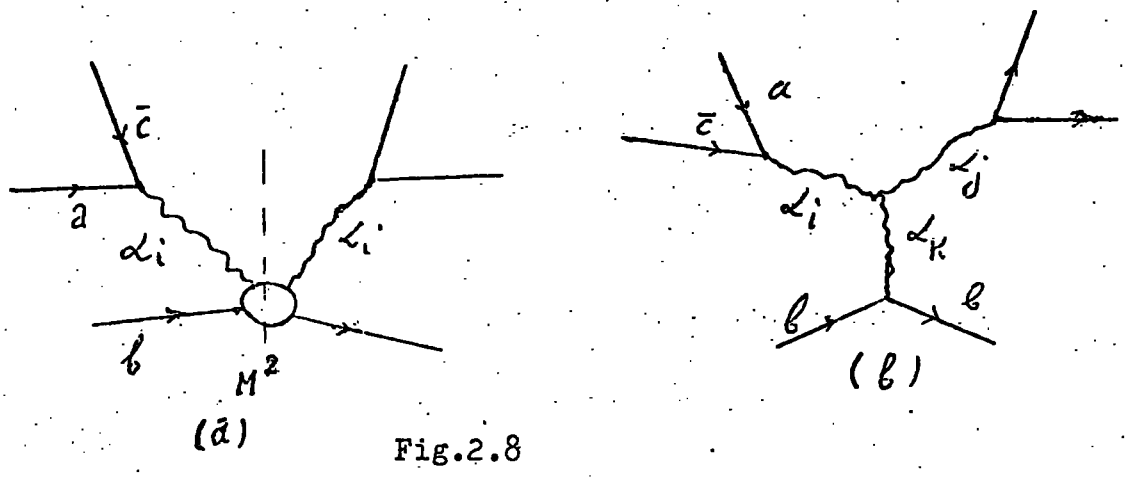

Fig.2.8

The normal Regge limit, represented in Fig.2.8(a), is defined by $s \longrightarrow \infty$, M^2, and t fixed. To obtain the asymptotic formula for the inclusive cross-section we proceed as follows. Consider the process in Fig.2.9.

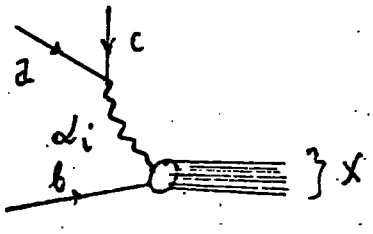

Fig2.9

Assuming that factorization holds, the asymptotic form for the process in Fig.2.9 is given by a Regge behaviour:

$$A(ab \longrightarrow cX) = \sum \gamma^i_{cab}(t)\gamma^i_{aM}(t)\xi_i(\cos\theta_t)^{\alpha_i(t)} \qquad (II.32)$$

where ξ_i is the signature factor $(\exp(i\alpha_i(t) + s)/\sin\pi\alpha_i)$, γ^i_{ac} represents the coupling between the particles a and c, and the Reggeon α_i, γ^i_{bM} represents the coupling between the particles b and X, and the Reggeon α_i, and $\cos\theta_t$ is defined by

$$\cos\theta_t = \frac{t^2 + t + (2s - m_a^2 - m_b^2 - m_c^2 - M^2) + (m_a^2 - m_c^2)(m_b^2 - M^2)}{4t\eta_{tac}\eta_{tbM}} \qquad (II.33)$$

where η_{tac} is defined

$$q_{tac} = \frac{1}{4t}(t - (m_a + m_c)^2)(t - (m_a - m_c)^2) \qquad (II.34)$$

and q_{tbM} is defined

$$q_{tbM} = \frac{1}{4t}(t - (m_b + M)^2)(t - (m_b - M)^2) \qquad (II.35)$$

Putting this into the optical theorem we find

$$f_1^{c,ab} = \frac{1}{s}\sum_X |A(ab \longrightarrow cX)|^2 =$$

$$= \frac{1}{s}\sum_{i,j} \gamma^i_{ac}\gamma^{*j}_{ac}\xi_i\xi^*_j(\cos\theta_t)^{\alpha_i(t)+\alpha_j(t)}\beta(t,M^2) \qquad (II.36)$$

where $\beta(t,M^2)$ is the discontinuity of of the forward elastic Reggeon particle amplitude. Replacing $\cos\theta_t$ by its asymptotic behaviour, we obtain

$$f_1^{c,ab} = \frac{1}{s}\sum \gamma^i_{ac}\gamma^{*j}_{ac}\xi_i\xi^*_j(s/M^2)^{\alpha_i(t)+\alpha_j(t)}\beta(t,M^2) \qquad (II.37)$$

The triple Regge limit is defined by $s \longrightarrow \infty, M^2 \longrightarrow \infty, s/M^2$ is large but fixed and t fixed. The asymptotic formula for $f^{c,ab}$ can easily obtained from a further Reggeisation of the discontinuity $\beta(t,M^2)$, where now M^2 is large. Thus one can write

$$f_1^{c,ab} = \frac{1}{s}\sum \gamma^i_{ac}\gamma^j_{ac}\xi_i\xi^*_j(s/M^2)^{\alpha_i(t)+\alpha_j(t)}\gamma^k_{ij}(t)\gamma^k_{bb}(t)\cdot$$
$$\cdot(M^2)^{\alpha_k(t)} \qquad (II.38)$$

where, as before, we assume that factorization holds.

II.5.2 Double Regge limit - Central Region.

Let us consider the region where $X \approx 0$. In this region the particle c is not slow in either the lab system, or in the projectile system. Thus we cannot consider it as a fragment of either of the particles a or b. In this region it is convenient to use the following set of variables u, t, and M^2 defined in (II.9), (II.8). In terms of these variables the double Regge limit is defined by s, $|t|$, and $|u|$ going to infinity and

M_c^2 fixed. Since both the sub-energies u and t are very large, one expects the amplitude to yield a double Regge behavior and so the inclusive cross-section $f_1^{c,ab}$ (see Fig.2.10) can be written

$$f_1^{c,ab}(t,u,M_c^2) = \frac{1}{tu}\sum \beta(M_c^2)\,|t|^{\alpha_i(0)}\,|u|^{\alpha_j(0)} = \sum \beta(M_c^2)\,|t|^{\alpha_i(0)-1}\,|u|^{\alpha_j(0)-1} \qquad (II.39)$$

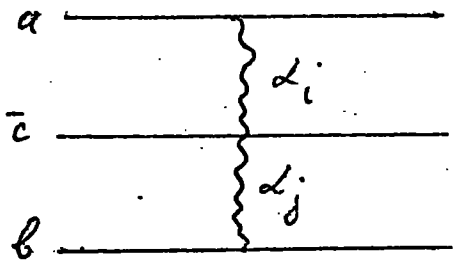

Fig.210

If we assume Pomeron dominance as before, we obtain

$$f_1^{c,ab} \simeq \beta(M_c^2) \qquad (II.40)$$

And remembering that $M^2 = m_c^2 + q_{cT}^2$, we find that the distribution function $f_1^{c,ab}$ is a function of q_{cT} only, in accordance with Feynman's prediction. Furthermore, assuming that the Pomeron is a factorizable pole, one can write

$$f(q_{cT}) \simeq \gamma_{aa}^{I\!P}\gamma_{bb}^{I\!P}\gamma_{cc}^{I\!P}(q_{cT}) \qquad (II.41)$$

and, since $\gamma_{aa}^{I\!P}\gamma_{bb}^{I\!P}$ determines asymptotically the magnitude of σ_{tot}^{ab}, the density ρ is given by

$$\rho = \frac{f_{ab}^{c}}{\sigma_{tot}^{ab}} = \gamma_c^{I\!P}(q_{cT}) \qquad (II.42)$$

a universal function depending only on the produced particles and not on the incident particles.

In the next chapter we shall consider the implication of the duality for such inclusive cross-section.

CHAPTER III

Duality and approach to scaling in single particle inclusive reactions

In chapter one we discussed dual diagrams for two-particle processes. The above scheme been successful in predicting several features of hadronic interactions. In particular the HF-conjecture predicts, via the optical theorem, the behaviour of the total cross-section. This success lead several authors to generalize the HF-conjecture to the case of single particle inclusive reactions. As in the case of total cross-sections, one expects the inclusive cross-section to depend upon the quantum numbers of the external particles involved. Unfortunately the generalization is not straight forward, because it is not clear what duality means other than for two-body reactions.

In chapter two we saw that the single particle inclusive reactions can be analysed in terms of six point functions. There involve several channels, and it is not clear how to apply duality scaling rules. Several criteria for the elimination of the secondaries (Reggeon contributions appear in the Mueller formula for the inclusive reactions (chapter II.)) have been proposed. In this chapter we discuss these criteria, their justification, and their region of validity.

III.1 Exoticity condition in the fragmentation region.

As we know from the second chapter there are mainly two important kinematical region to be considered, the fragmentation and the pionization regions. We present here the different

criteria which have been proposed for early scaling in the fragmentation region.

The first approach to the problem was by Chan[15] et al, who argued that the criteria obtained in the case of 4-point functions are good enough to be generalized to the six point functions. This is because, in the fragmentation region, the cluster $a\bar{c}$ is clearly separated from particle b, and thus can be considered as a pseudoparticle, provided the quantum numbers of $a\bar{c}$ are not exotic.

From the previous discussion we see that for two-body interactions σ_{tot} is determined by the forward two-particle elastic amplitude, and an exotic direct channel is enough to eliminate the secondaries, where as in the case of the single-particle inclusive reaction the distribution function is determined in terms of the three-body forward elastic amplitude Thus Chan et al suggest that an exotic three-body direct channel $(ab\bar{c})$ is a sufficent criterion for the elimination of the secon--daries. Their criterion works for Kp- interactions, since for $K^+ + p \longrightarrow \pi^{\pm} +$ anything, which is exotic in the direct channel has has an enegy independent distribution function, whereas the reaction $K^- + p \rightarrow \pi^{\pm}$ + anything which is not exotic in the direct channel, has a strong energy dependence.

Another criterion has been suggested by Ellis et al[16]. They argue that the Chan criterion is a necessary condition for the elimination of the secondary trajectories in the three-body reactions, but not sufficient. It neglects the effect of the two-body channel, which if not exotic, contributes to the dis-

-continuity of the three-body channel. Moreover, for the react-ions $\pi^{\pm}+p \rightarrow K^{+}+$anything, where $ab\bar{c}$ is exotic in both cases, they show that factorization makes the above criterion inconsistant. It demands the vanishing of the contributions of individual Regge trajectories rather than exchange degeneracy between them. To see this we write the Regge description for the above reaction as follows

$$f_1^{K^+,\pi^{\pm}p} = \beta_R(P_{cL},P_{cT}) + (\beta_f(P_{cL},P_{cT}) \pm \beta_f(P_{cL},P_{cT}))M^{-1/2} \qquad \text{(III.1)}$$

where β_f and β_f are the contributions of the f and f'-trajectories exchanged in the above reactions. Thus satisfaction of Chan criterion in both reactions demands the vanishing of $\beta_f \pm \beta_f$, which implies the vanishing of β_f and β_f separately. They con-clude that even if the Chan criterion is sufficient it is certainly not necessary.

In the fragmentation region of a into c, both $(\bar{c}b)$ and $(a\bar{c})$ channels are below the thresholds, so the relevent two-particle channel effect can come only from the (ab) channel. Therefore as a sufficient criterion for the flatness of the distribution function they suggest, that in addition to $(ab\bar{c})$ exotic, one needs (ab) exotic.

A different viewpoint, within the framework of dual per-turbative scheme, has been proposed by Einhorn, Green, and Virasoro[17] (EGV).

For process $a+b+\bar{c} \longrightarrow a+b+\bar{c}$, in the fragmentation region of a into c, the leading contribution comes from the diagrams which have a non-vanishing discontinuity in the $ab\bar{c}$ channel, and

a Reggeon or Pomeron in the $b\bar{b}$ channel. In Fig.3.1 we draw all the relevant primitive planar diagrams.

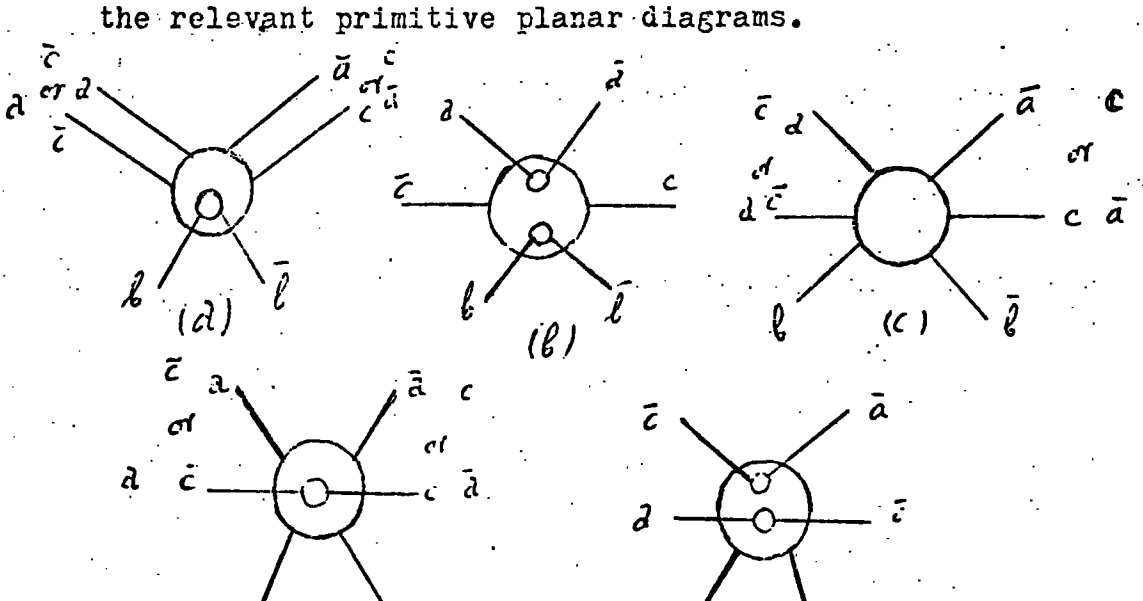

Fig.3.1

In chapter two we see that the Muller expression for the distribution function contains two parts, a scaling part which is built up from the Pomeron in the $b\bar{b}$ channel, and a nonscaling part which is built up from the contribution of a Reggeon in the same channel. Thus to obtain early scaling, the main task will be to eliminate diagrams which have a Reggeon in the $b\bar{b}$-channel. Diagrams in Fig.3.1(a) and (b) are irrelevant to our discussion. They do not contribute to the nonscaling part, since there is no Reggeon in the $b\bar{b}$-channel.

All the other diagrams in Fig.3.1 have a Reggeon in the $b\bar{b}$ channels, and contribute to the nonscaling part. Applying the rules obtained in chapter one, EGV come to the conclusion that for early scaling it is necessary and sufficient to have (ab) and ($b\bar{c}$) exotic. Indeed it is straightforward to check that the above criteria will eliminate all the relevant diagrams in

Fig.3.1.

EGV expect this criterion to work in the whole fragmen-
-tation region. They expect in certain limited regions of phase space the other criteria to be good as well. Thus for example in the triple Regge limit, the tree diagrams, Fig.3.1(c), are expected to be the dominant non-scaling diagrams. To the extent that Fig.3.1(c) does dominate in this region, the condition (abc̄) exotic is enough to ensure early scaling.

In the opinion of Chan et al the tree diagrams are the dominant ones in the whole fragmentation region. They suggest that all the other diagrams in which a and c are not adjacent, have vanishing limits. In other words, in the fragmentation limit of a into c, $\beta_R \simeq 0$ (where β_R has been defined in chapter II, in the content of the Muller expansion of the distribution function in the fragmentation region) for all those diagrams in which a and c are not resonant. Thus according to Chan, within the above approximation (abc̄) exotic is sufficient criterion for the early scaling in the whole fragmentation region. However it is known experimentally that the Pomeranchukon has coupling of the same order as the Reggeons. Thus there is no reason why β_R should 0 if a Pomeranchukon contributes to the ac̄ channel.

We conclude this section by discussing a recent proposal by Tye and Veneziano[18]. Following the argument given in chapter I, for the decomposition of the total cross section into a sum of one and two resonance components, one finds that for the single particle inclusive cross-section, seven components can be obtained. In Fig.3.2 we display all those components which

contribute to the production amplitude A(a + b ⟶ c + X). Multi-plying each component by its complex conjugate and summing over all X (X represents anything produced except c), one obtains the seven components contributing to the σ_{tot}. These seven comp-onents are in fact identical with some of those for planar duality Fig.3.1

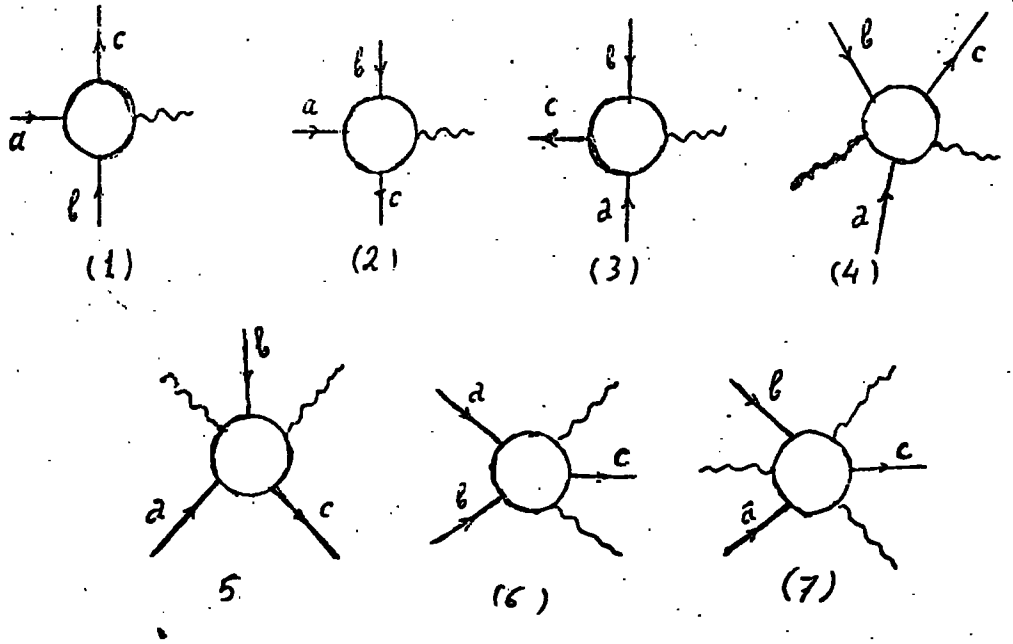

Fig.3.2

In obtaining the seven components, we leave out the diff-ractive part A_D, which we discuss later, and ignore interfer.-ence terms. Then the inclusive cross section is given by

$$E_c\frac{d^3\sigma}{dP_c^3} = \sum_{i=1}^{7}\left(E_c\frac{d^3\sigma}{dP_c^3}\right)_i \qquad \left(E_c\frac{d^3\sigma}{dP_c^3}\right)_i > 0 \qquad \text{(III.2)}$$

where $\left(E_c\frac{d^3\sigma}{dP_c^3}\right)_i$ can be writen as follows

$$\left(E_c \frac{d^3\sigma}{dP_c^3}\right)_i = \beta_i(X,P_{cT}) + \tilde{\beta}_i(X,P_{cT}) s^{\alpha(0)-1} \qquad \text{III.3}$$

The characteristic of each component has been summarized in table -1-

Table -1-

Component	Channel required to be non-exotic	Vacuum quantum numbers in	Non-scaling piece	Scaling piece
1	ab, $b\bar{c}$, $ab\bar{c}$	none	$\tilde{\beta}_1$	$\beta_1 = 0$
2	ab, $a\bar{c}$, $ab\bar{c}$	none	$\tilde{\beta}_2$	$\beta_2 = 0$
3	$b\bar{c}$, $a\bar{c}$, $ab\bar{c}$	none	$\tilde{\beta}_3$	$\beta_3 = 0$
4	ab	$c\bar{c}$	$\tilde{\beta}_4$	$\beta_4 = 0$
5	$b\bar{c}$	$a\bar{a}$	$\tilde{\beta}_5$	β_5 $x<0$ $\beta_5 = 0, x>0$
6	$a\bar{c}$	$b\bar{b}$	$\tilde{\beta}_6$	β_6 $x>0$ $\beta_6 = 0, x<0$
7		$a\bar{a}$, $b\bar{b}$, $c\bar{c}$	$\tilde{\beta}_7$	β_7

From the above table we see that for the elimination of the secondary contribution all the channels need to be exotic.

To end this section we summarize all the criterion for the elimination of the secondaries in the fragmentation region of a into c.

1. Chan et al $ab\bar{c}$ exotic.
2. Ellies et al $ab\bar{c}$ and ab exotic.
3. Einhorn et al ab and $\bar{c}b$ exotic.
4. Tye and Veneziano all the channel is to be exotic.

III.2 Exoticity condition in the central region.

In chapter II we showed that pionization is expected to be valid only when both u and t are large, keeping $\frac{ut}{s}$ = constant. The main diagrams contributing to the nonscaling limit

are those which have Reggeon-Reggeon or Reggeon-Pomeron exchange in $a\bar{a}$ and $b\bar{b}$ channels. This is easy to see from Muller's-Regge expansion of $f^{c,ab}(P_{cT},P_{cL},s)$ eq (II.39). The relevant diagrams are shown in Fig.3.2

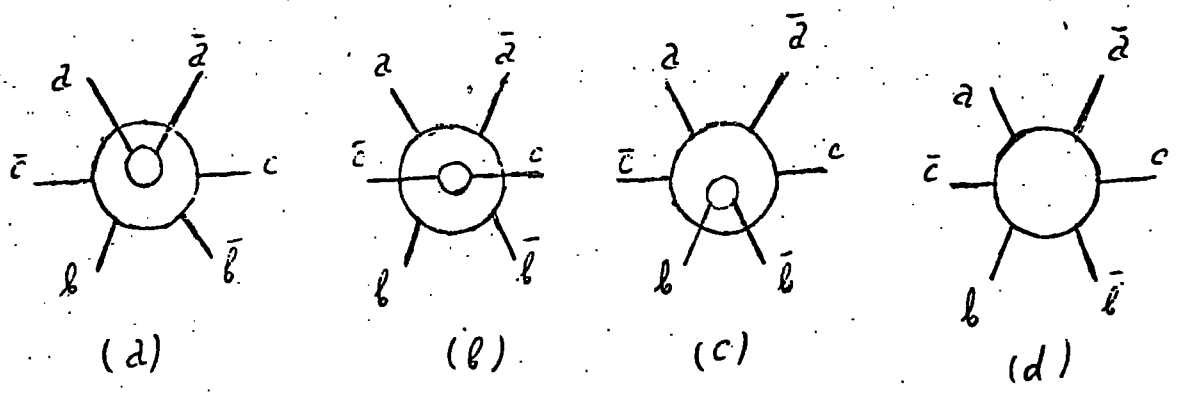

Fig.3.2

The condition for the elimination of these diagrams is shown in table 2 given by EGV.

Table -2-

Diagrams as labelled in Fig.3.4	Exchanged Regge singularity in $a\bar{a}$	in $b\bar{b}$	Condition for the absence of the contribution
a	$\mathbb{P}$	R	$b\bar{c}$ exotic
b	R	R	ab exotic
c	R	$\mathbb{P}$	$a\bar{c}$ exotic
d	R	R	$a\bar{c}$ or $b\bar{c}$ or $ab\bar{c}$ exotic

From table 2 we find that the condition for the elimination of all these diagrams is ab, $a\bar{c}$, and $b\bar{c}$ exotic. In fact not all these diagrams will be of equal importance. The asymptotic behaviour of $f(X,s,\ell_{iT})$ given in eq (II.39), is

$$f(X,s,\ell_{iT}) \sim |u|^{\alpha_i - 1} \quad |u|^{\alpha_i - 1} \qquad \text{(III.4)}$$

From the above we see that the contribution of the diagrams(a) and(c) to $f(X,s,\gamma_{cT})$ is $|t|^{-1/2}$, while the contribution of the diagrams (b) and (d) $|t|^{-1/2}|u|^{-1/2}$. And if we consider the limit $P_{//c} = 0$ then u and t are both proportional to $s^{1/2}$. Then we see that the two terms (a) and (c) go like $s^{-1/4}$, while (b) and (d) go like $s^{-1/2}$ and at a very high energy become negligible by comparision with (a) and (c). In this case to eliminate the secondaries it is sufficient to have $a\bar{c}$ and $b\bar{c}$ exotic.

CHAPTER IV

Experimental tests of scaling

IV.1 Scaling and tests of the exoticity criterion in the fragmentation region.

In chapter II we defined Feynman and Yang et al scaling in inclusive reactions. We see that scaling means the independence of the inclusive cross-section of the energy variable asymptotically, and moreover in the pionization region it means independence of the scaling variable X. In Fig.2.1, and 2.3 we show some evidence for the scaling. Fig.2.1 illustrates the transverse momentum distribution at X = 0 observed at different ISR energies together with distributions at accelerator energies while Fig.2.3 shows the inclusive cross-section for $pp \longrightarrow pX$ and $pp \longrightarrow \pi^+ X$ as a function of the Feynman variable X for a fixed transverse momentum at two different energies. In both cases the inclusive cross-section is obviously independent of the energy. Further illustrations are given in Figs.4.1 and 4.2, where Fig. 4.1 shows the transverse momentum distribution in $pp \longrightarrow \pi^+ X$ reaction for different values of X at two different energies, and Fig.4.2 shows the inclusive distribution of rays at very low transverse momentum for different values of the scaling variable X. These two diagrams also clearly demonstrate scaling.

Now we proceed to a more detailed analysis of the scaling hypotheses. In the table-3- we classify each reaction and also summarize the existing experimental data. Our survey is not complete, being based predominantly on 1972 experimental data, but the main aim is to show sufficient evidence either to support or to discredit the varios criteria for scaling.

Table -3-

Process	Channels				Predictions				Experimental	Early scaling		Notes
	$ab\bar{c}$	ab	$a\bar{c}$	$b\bar{c}$	1	2	3	4	Figs.	Frag	Pion	
$pp \longrightarrow \pi^- X$	E	E	N	N	S	S	NS	NS	4.3, 4.4, 4.5,	?	S	1, 2, 3 and 4
$pp \longrightarrow \pi^+ X$	E	E	N	N	S	S	NS	NS	4.6, 4.7,	S	S	
$pp \longrightarrow \Lambda X$	E	E	N	N	S	S	NS	NS	4.8	NS	-S	5, 6 7, 8
$\pi^+ p \longrightarrow \pi^- X$	E	N	N	E	S	NS	NS	NS	4.9(a)	S	N	9, 9 10
$\pi^+ p \longrightarrow \pi^+ X$	N	N	N	N	NS	NS	NS	NS	4.9(b)	N	S	11,12
$pp \longrightarrow pX$	N	E	N	N	NS	NS	NS	NS	4.10; 4.11	S	S	13,14
$pp \longrightarrow \bar{p}X$	E	E	E	E	S	S	S	S	4.11, 4.12	NS	NS	15,16
$p\bar{p} \longrightarrow K^+ X$	E	E	N	N	S	S	N	N		S(approx)		
$pp \longrightarrow K^- X$	E	E	E	E	S	S	S	S		NO		

Where E represents exotic, N nonexotic, S scaling, NS nonscaling, and by 1, 2, 3, and 4 we refer to the Chan, Ellies, Einhorn, and Tye criterion respectively.

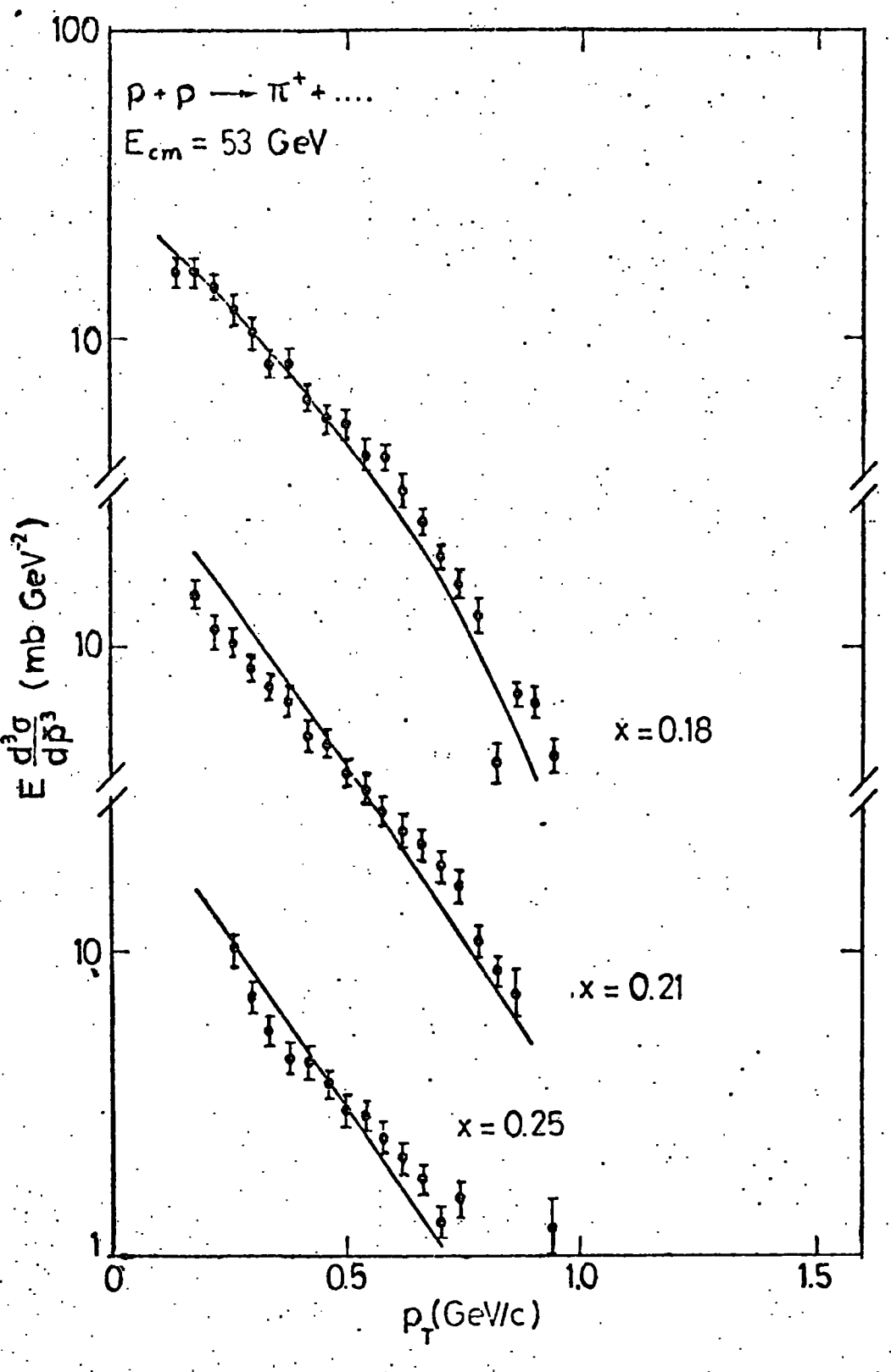
100
p + p → π⁺ + ...
E_cm = 53 GeV
10
10
10
1
E d³σ/dp³ (mb GeV⁻²)
x = 0.18
x = 0.21
x = 0.25
0
0.5
1.0
1.5
p_T (GeV/c)

Fig.4.1

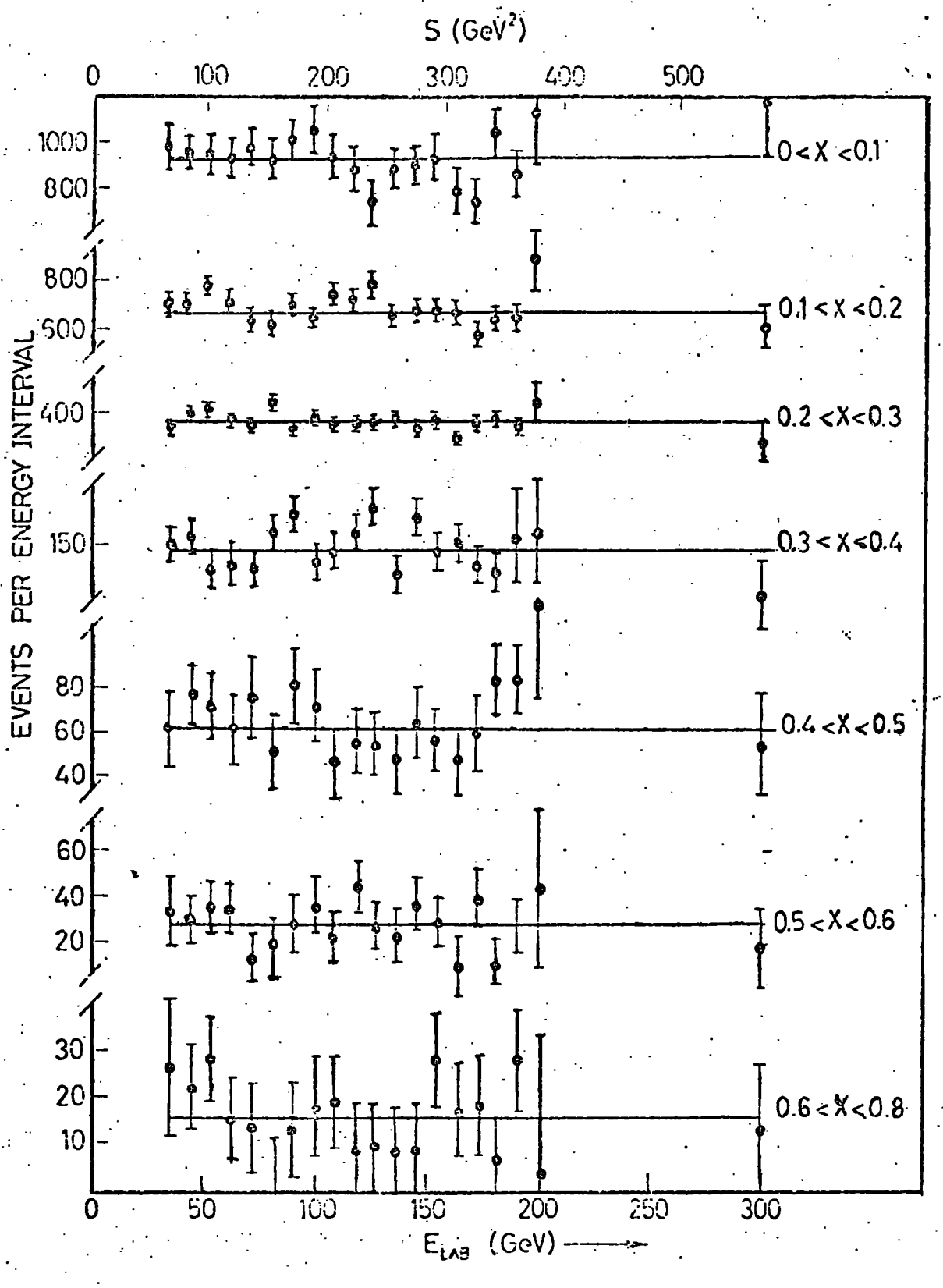
S (GeV²)
0
100
200
300
400
500
1000
800
800
500
400
150
80
60
40
60
40
20
30
20
10
0<X<0.1
0.1<X<0.2
0.2<X<0.3
0.3<X<0.4
0.4<X<0.5
0.5<X<0.6
0.6<X<0.8
EVENTS PER ENERGY INTERVAL
0
50
100
150
200
250
300
E_LAB (GeV) ⟶

Fig.4.2

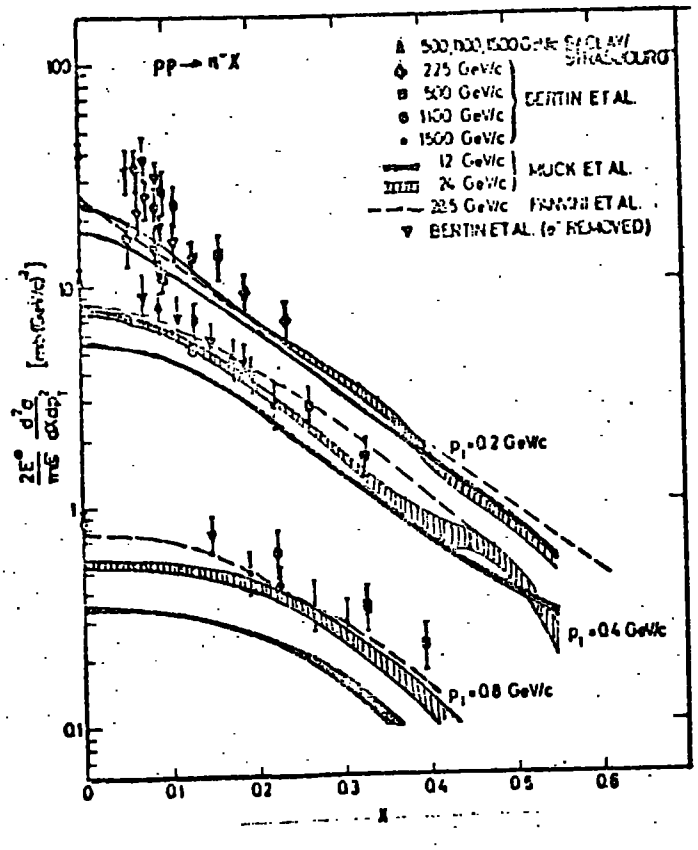
PP → π⁻X
500,1100,1500 GeV/c SACLAY/STRASBOURG
225 GeV/c
500 GeV/c
1100 GeV/c
1500 GeV/c
BERTIN ET AL.
12 GeV/c
24 GeV/c
MUCK ET AL.
28.5 GeV/c
BERTIN ET AL. (e⁻ REMOVED)
p_t=0.2 GeV/c
p_t=0.4 GeV/c
p_t=0.8 GeV/c
x

Fig.4.3

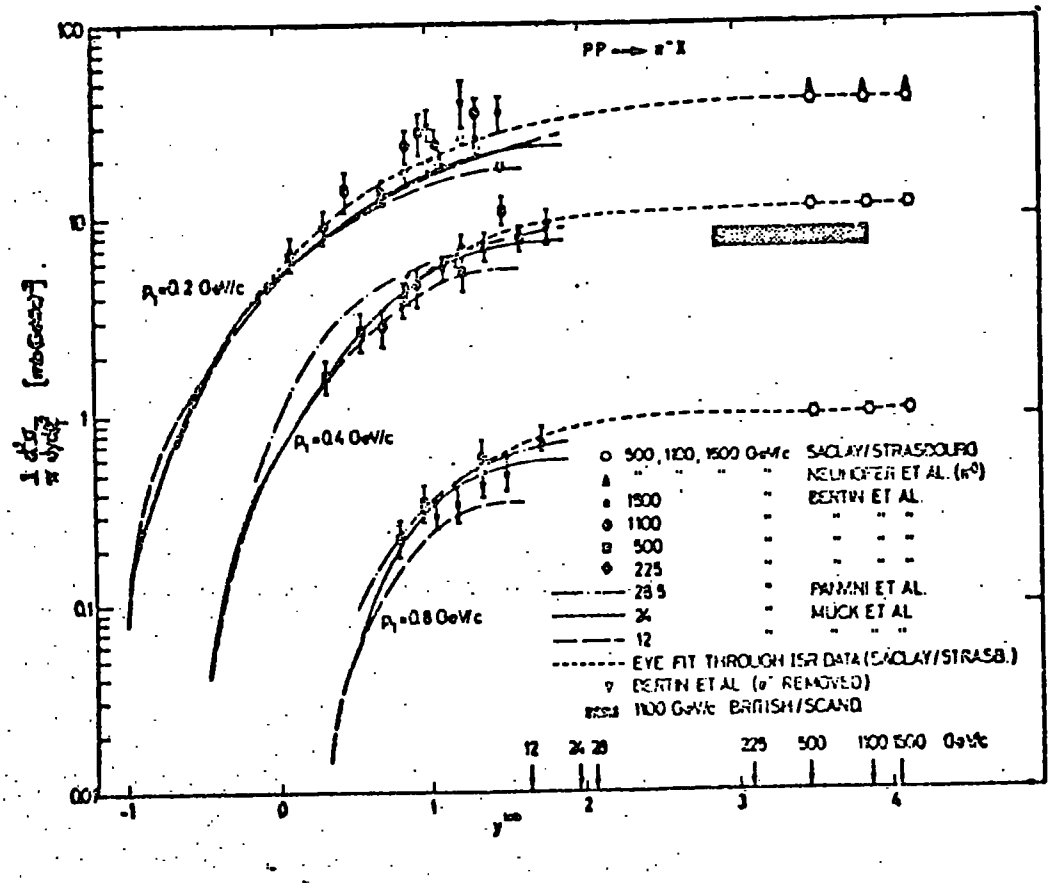
PP → π⁻X
p_t=0.2 GeV/c
p_t=0.4 GeV/c
p_t=0.8 GeV/c
500, 1100, 1500 GeV/c SACLAY/STRASBOURG
1500
1100
500
225
28.5
24
12
BERTIN ET AL.
PANNI ET AL.
MUCK ET AL
EYE FIT THROUGH ISR DATA (SACLAY/STRASB.)
BERTIN ET AL (e⁻ REMOVED)
1100 GeV/c BRITISH/SCAND
12 24 28 225 500 1100 1500 GeV/c
y*

Fig.4.4

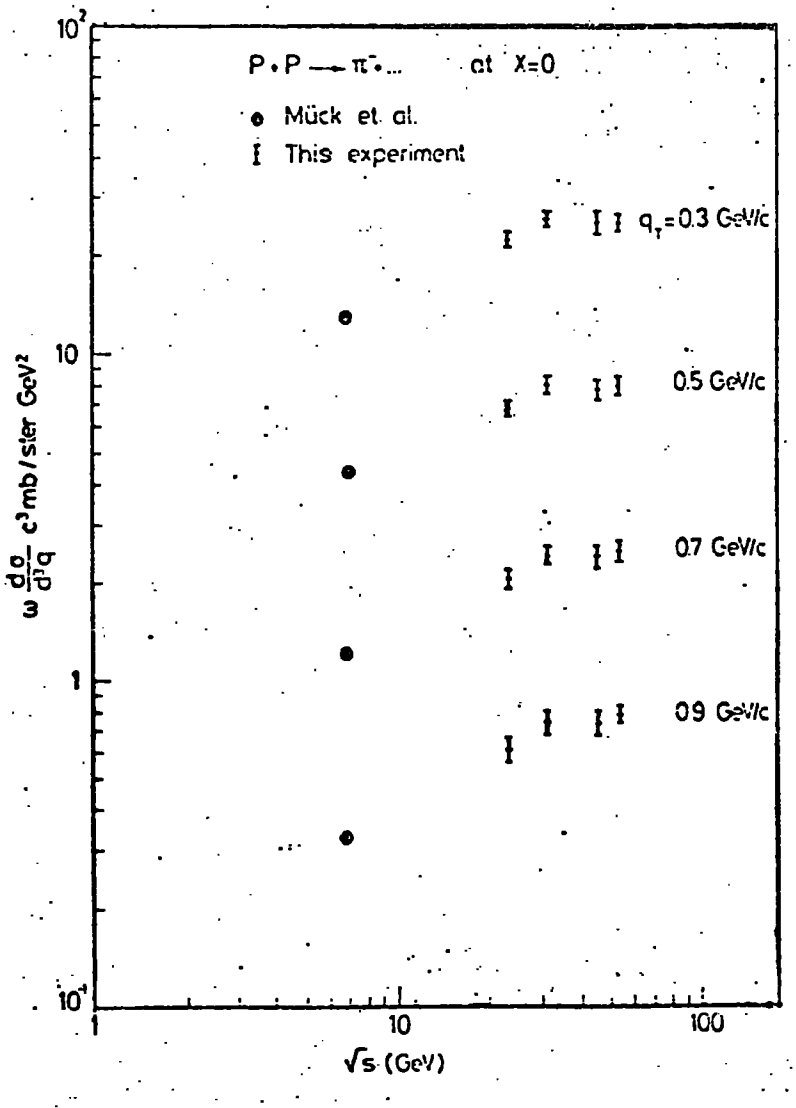
P + P → π⁻ + ... at X=0
Mück et al.
This experiment
q_T=0.3 GeV/c
0.5 GeV/c
0.7 GeV/c
0.9 GeV/c
$\omega \frac{d\sigma}{d^3q}$ c³mb/ster GeV²
$\sqrt{s}$ (GeV)
10^2
10
1
10^{-1}
1
10
100

Fig.4.5

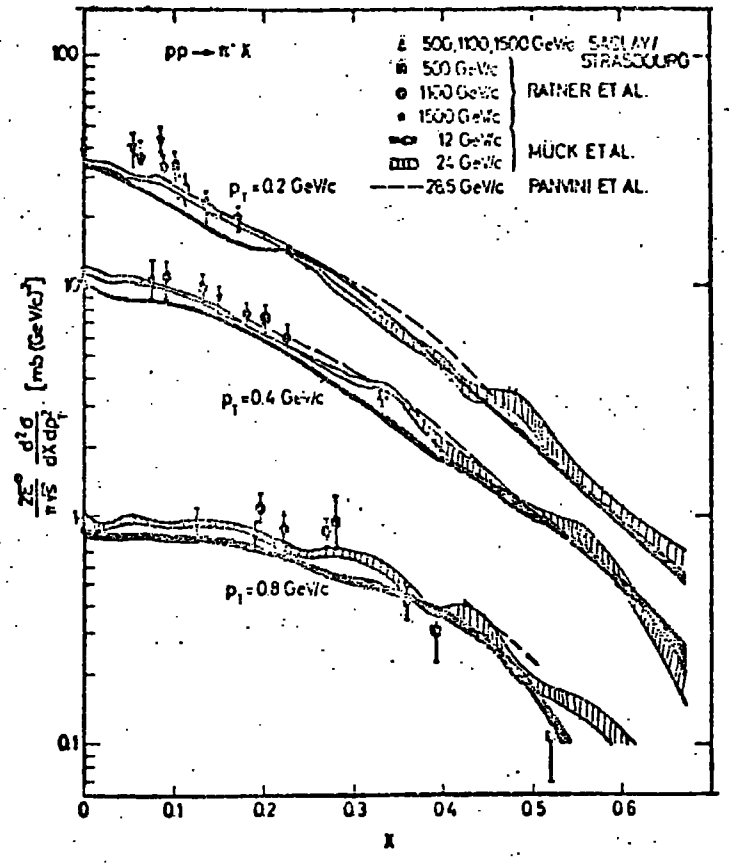
pp → π° X
500, 1100, 1500 GeV/c SACLAY/STRASBOURG
500 GeV/c
1100 GeV/c
1500 GeV/c
RATNER ET AL.
12 GeV/c
24 GeV/c
MÜCK ET AL.
26.5 GeV/c
PANVINI ET AL.
p_T = 0.2 GeV/c
p_T = 0.4 GeV/c
p_T = 0.8 GeV/c
X

Fig.4.6

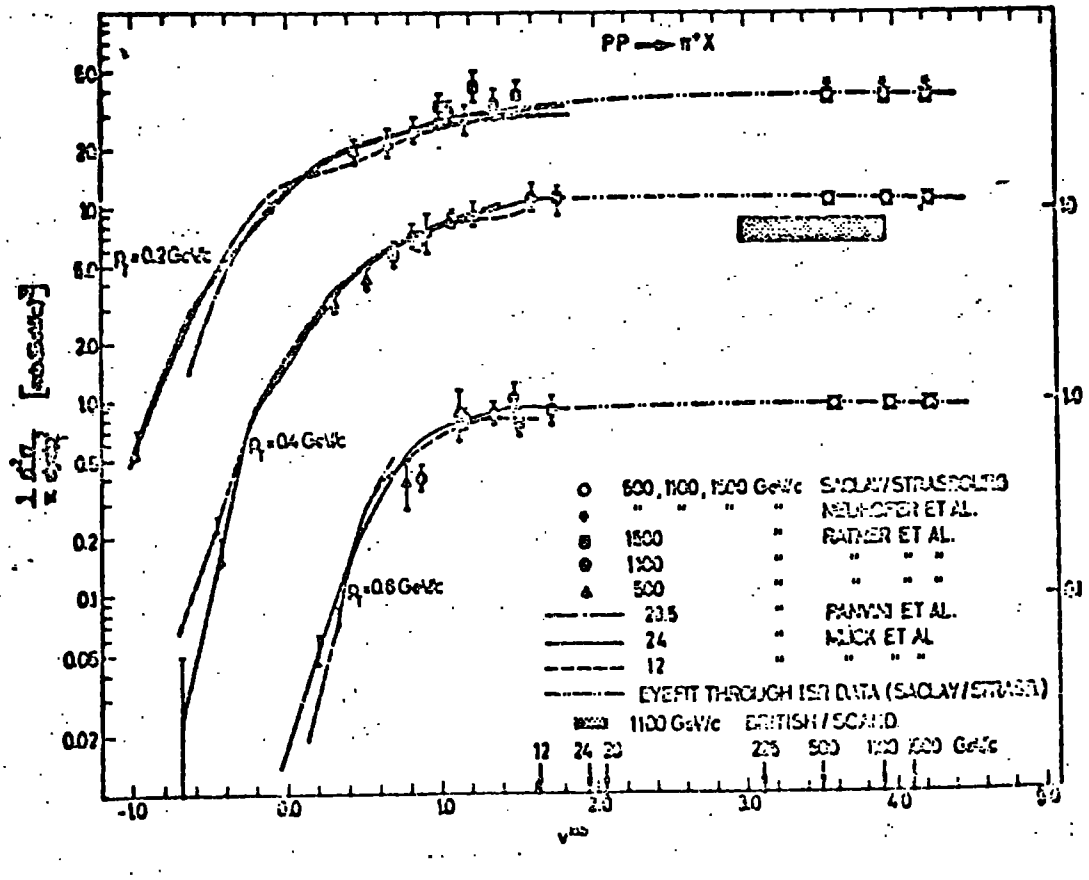
PP → π°X
p_T = 0.2 GeV/c
p_T = 0.4 GeV/c
p_T = 0.8 GeV/c
600, 1100, 1500 GeV/c SACLAY/STRASBOURG
NEUHOFER ET AL.
1500 " RATNER ET AL.
1100 " " " "
500 " " " "
23.5 " PANVINI ET AL.
24 " MÜCK ET AL.
12 " " " "
EYEFIT THROUGH ISR DATA (SACLAY/STRASB.)
1100 GeV/c BRITISH/SCAND.
12 24 26 235 500 1100 1500 GeV/c

Fig.4.7

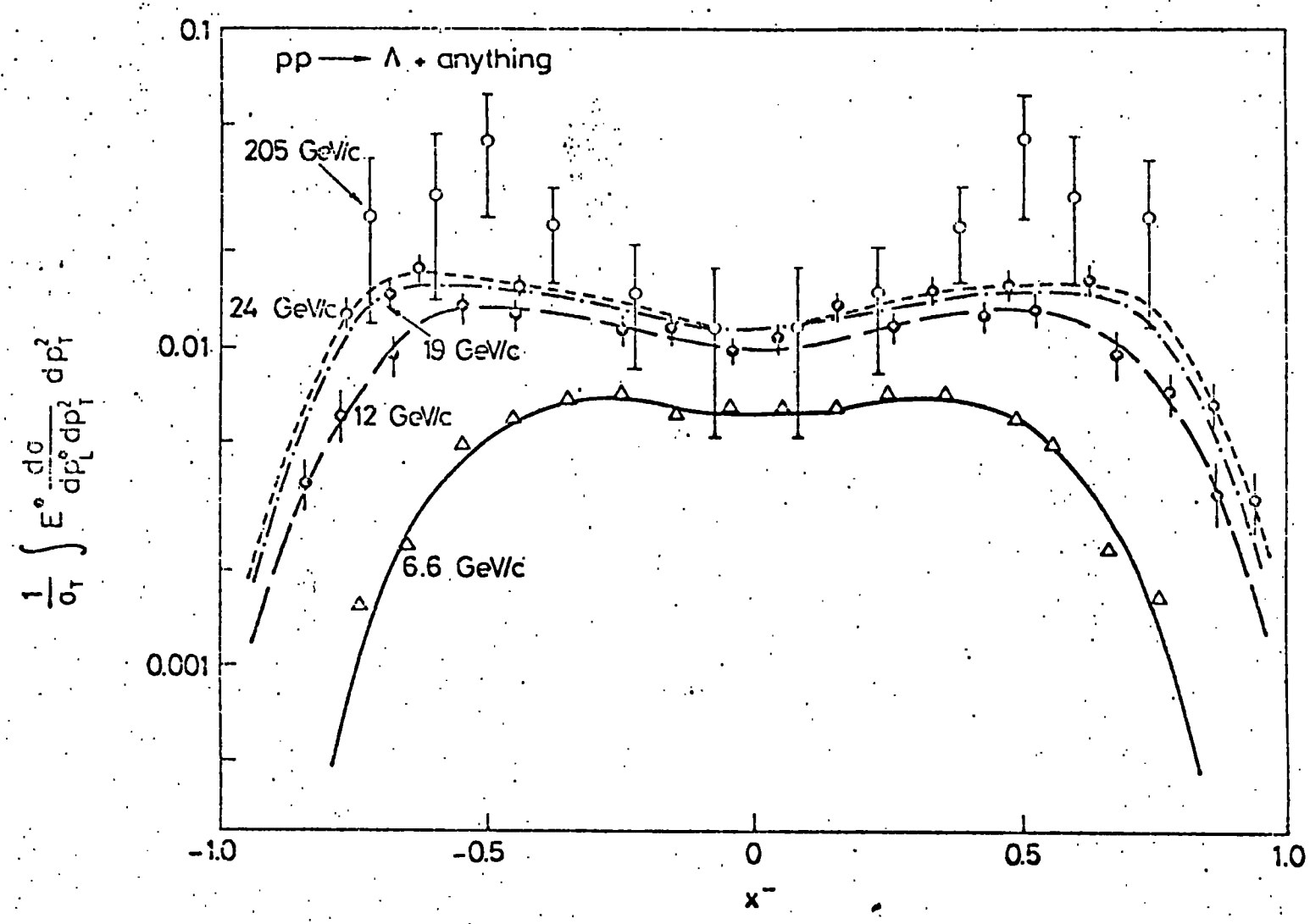
pp ⟶ Λ + anything
205 GeV/c
24 GeV/c
19 GeV/c
12 GeV/c
6.6 GeV/c
0.1
0.01
0.001
-1.0
-0.5
0
0.5
1.0
x⁻
$\frac{1}{\sigma_T}\int E^* \frac{d\sigma}{dp_L^* dp_T^2} dp_T^2$

Fig.4.8

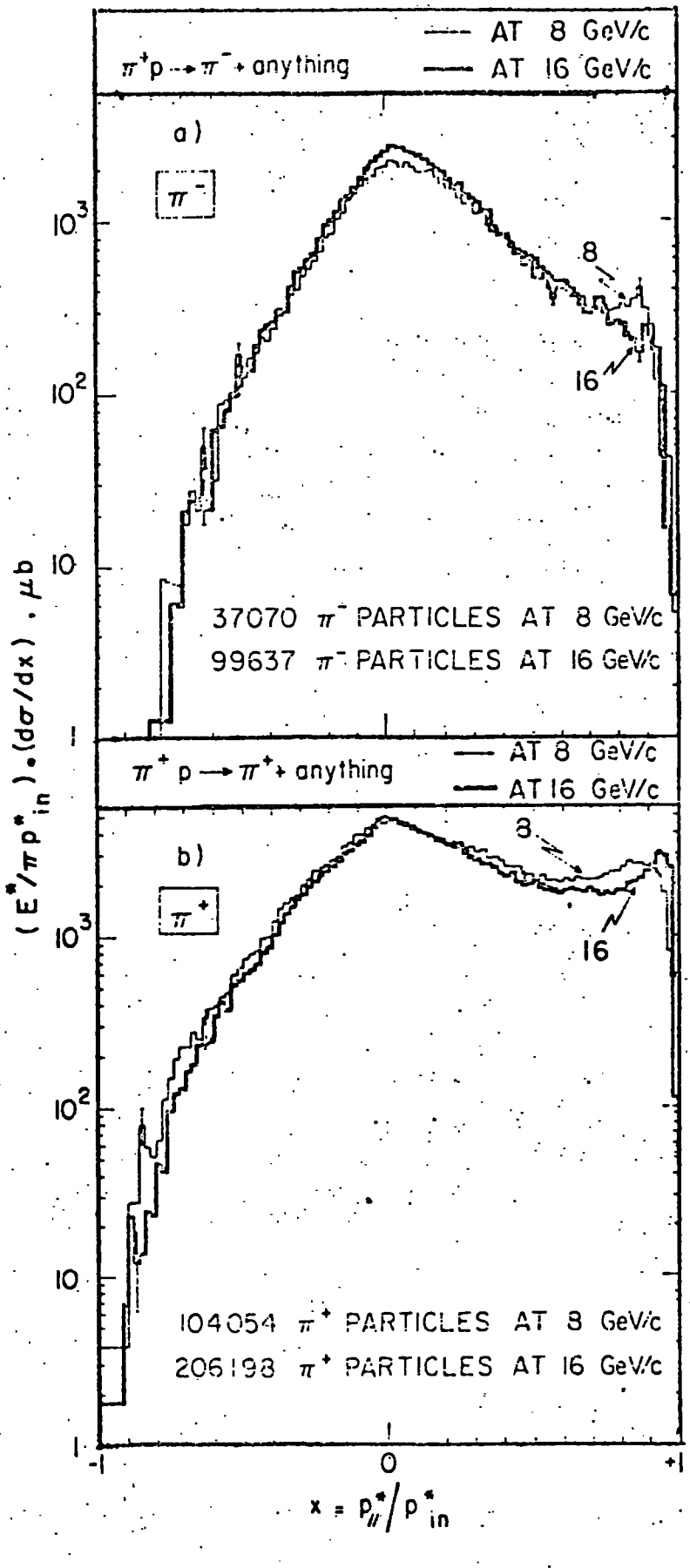
AT 8 GeV/c
AT 16 GeV/c
$\pi^+ p \to \pi^- +$ anything
a)
π^-
8
16
37070 π^- PARTICLES AT 8 GeV/c
99637 π^- PARTICLES AT 16 GeV/c
$\pi^+ p \to \pi^+ +$ anything
AT 8 GeV/c
AT 16 GeV/c
b)
π^+
8
16
104054 π^+ PARTICLES AT 8 GeV/c
206198 π^+ PARTICLES AT 16 GeV/c
10^3
10^2
10
1
-1
0
+1
$(E^*/\pi p^*_{in}) \cdot (d\sigma/dx) \cdot \mu b$
$x = p^*_{//}/p^*_{in}$

Fig 4.9

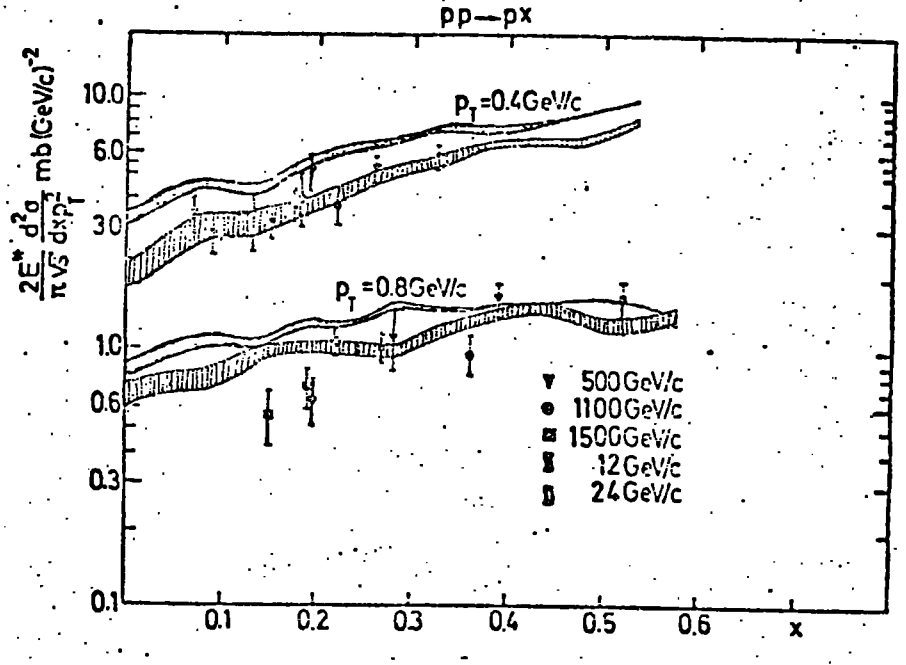

Fig.4.10

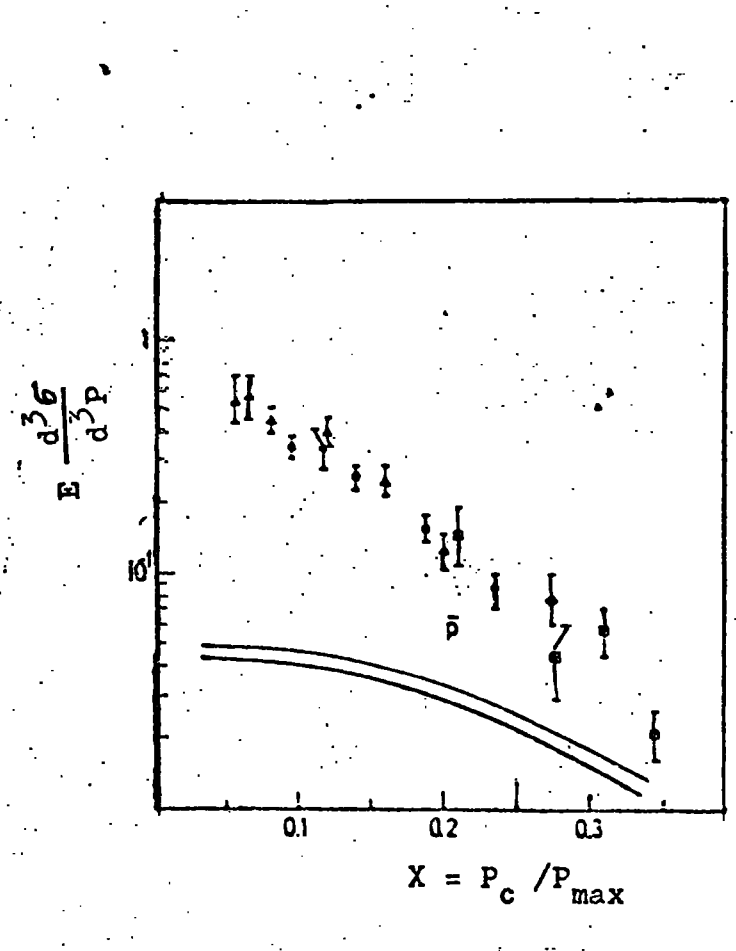

Fig.4.12

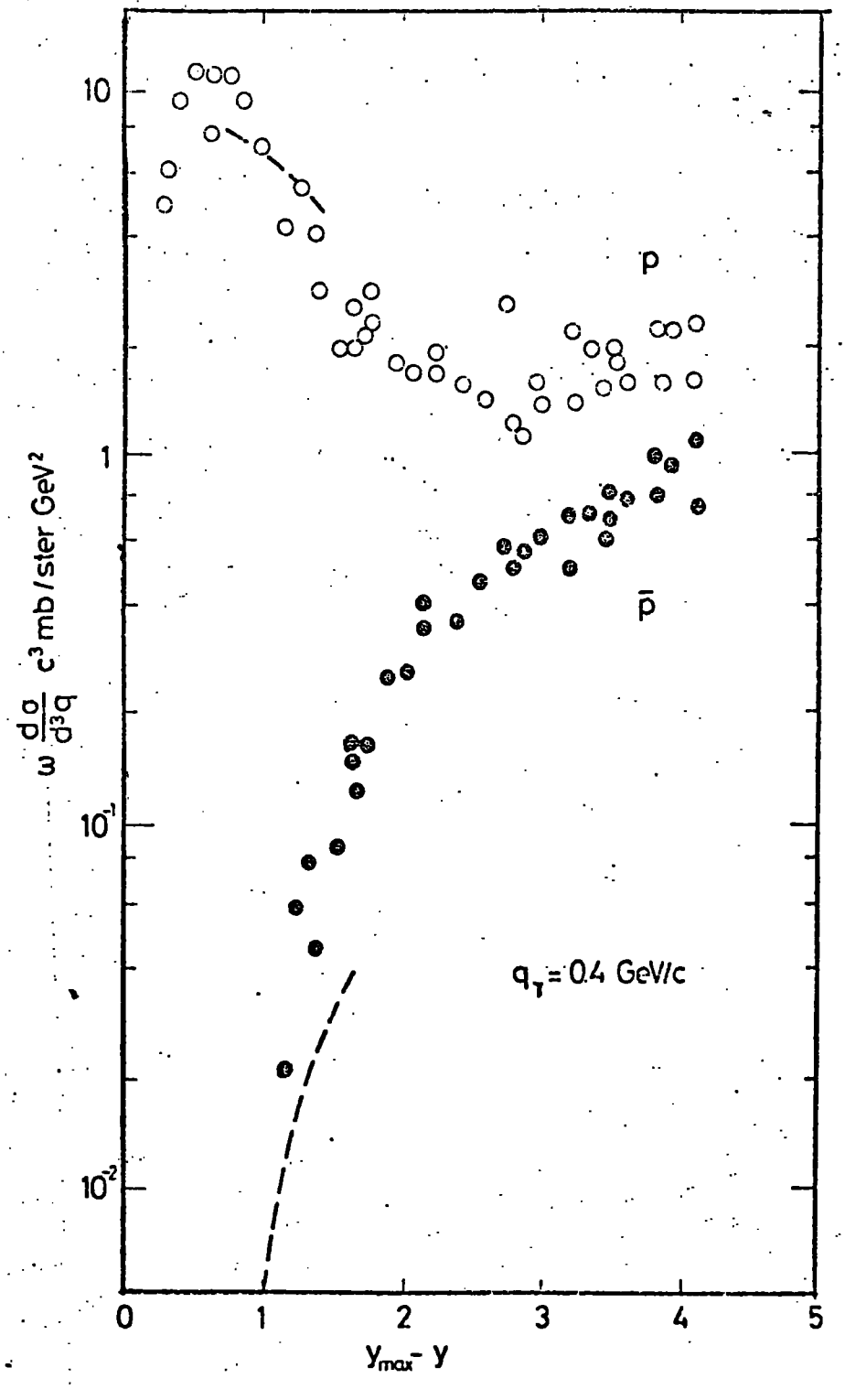
10
1
10^{-1}
10^{-2}
$\omega \frac{d\sigma}{d^3q}$ c^3 mb/ster GeV^2
p
$\bar{p}$
q_T = 0.4 GeV/c
0
1
2
3
4
5
$y_{max} - y$

Fig.4.11

Notes

1- Ih the fragmentation region the π^- inclusive cross-section (Fig.4.3)is rising at accelarator energies especially for large P_T, but scales in the ISR energy range. While the π^+ inclusive cross-section (Fig.4.6) is independent of the incident energies from 12 to 1500 Gev/c.

2- In the pionization region close to X=0 scaling is observed at ISR in both cases. This can also be seen from the rapidity plot, Figs.4.4 and 4.7, where the plateau is already developed. It is also evident that π^+ is approaching the scaling limit much faster than π^- in both the pionization and the fragmentation regions.

3- From Fig.4.5 we see that the π^- distribution rises by a factor of 2 between 20 and 1000 Gev in the lab system, but the rise is small for energies above 1000 Gev(Notes: In Fig.4.5 the plot is in terms of center of mass energies.).

4- We prefer to assume scaling in the case of π^+ rather then π^-, the π^- distribution function scales only partialy.

5- There is no early scaling in the fragmentation region. The rise continues up to 205 GeV/c.

6- In the X=0 region the scaling limit may already have been reached.

7- The rise in the fragmentation region may be compitable with $s^{-1/2}$ (not conclusive)in accordance with Muller's analysis.

8- Early scaling is observed in the fragmentation region

9- Within the above energy limit there is no scaling in the pionization region.

10- The scaling limit is approached from above.

11- There is no early scaling(or at least within the 8 and 16 GeV/c) .

pionization region.

10- The scaling limit is approached from above.

11- There is no early scaling (or at least within the 8 and 16 GeV/c) in the fragmentation region.

11- Surprisingly there is scaling in the pionization region, within the 8 to 16 GeV/c the distribution function does not change.

13- For small transverse momenta scaling holds approximately from 24 GeV/c up to ISR energies in both fragmentation and pionization region. For large P_T(=0.8 GeV/c)scaling holds up to X=0.2, but close to the pionization region there is no scaling.

14- The inclusive cross-section is falling. This also can be seen from Fig.4.11 .

15- There is no scaling in both the fragmentation and pionizat-ion regions.

16- From Fig4.12 we see that the inclusive reaction is rising in the pionization region.

Finally we try to draw some conclusions from the above situation. From the data and the theoretical predictions we see that there is no wide support for any of the criteria suggested so far. There may be one or two cases which support each of the criteria, but even in our short review of the experimental situation we find at least one good piece of evidence which discredits each of the criteria. Moreover, the inclusive react-ion $pp \rightarrow \bar{p}X$ take all the criteria by surprise, since it does not scales, contrary to all the theoretical predictions. We leave

further comment to the next chapter where we shall also discuss another problem which arises from the above data, the fact that the approach to scaling is from below, rather than from above as we expect.

CHAPTER V

The approach to scaling, and conclusions.

V.1 The approach to scaling.

In chapter IV, from the experimental data, we see that sometimes the single particle inclusive cross-section is rising to its asymptotic limit.

None of the planar diagrams will give us this sort of feature. In seven-component theory, for example,we naively expect all the components to be positive, since they build up from the square of the production amplitude.

Several solutions to this problem have been advocated:
1) The first was proposed by Tye and Veneziano.They believe that the answer lies within the seven components and so one does not need to to involve the so far neglected, diffractive terms and the interference terms.

Using sum rules and assuming the strong HF-conjecture they found that some of $\beta_i(X,P_T)$ in III.3 must have a negative sign depending on the choice of phase space and/or of c. Here we give a brief sketch of the approach used and give the results[19].

The sum rules which have been used are

$$(P_a + P_b)_\mu \sigma_{ab} = \sum_c \int dP_c P_{c\mu} f^{c,ab} \qquad (V.1)$$

where P_a, P_b, and P_c are the four momenta of the particles a, b and c, respectively. This sum rule is a statement of four-momentum conservation.

Charge conservation gives similarly

$$(Q_a + Q_b)\sigma_{ab} = \sum \int dP_c Q_c \, f^{c,ab} \qquad (\bar{V}.2)$$

Equation $\bar{V}.1$ for the $\mathcal{N} = 0$ component can be written as.

$$2\sigma_{ab} = \frac{1}{2} \sum \int dP_{cT} dX \, f^{c,ab} \qquad (\bar{V}.3)$$

Writing the σ_{tot} in the form

$$\sigma_{tot} \simeq C_{ab} + \tilde{C}_{ab}(s/s_o)^{-1/2} + \ldots . \qquad (\bar{V}.4)$$

and combining III.2 with $\bar{V}.3$ one gets

$$2C_{ab} = \frac{1}{2} \sum_{i=1}^{7} \sum_{c} \int dP_{cT} dX \beta_i(X, P_{cT}) \qquad (\bar{V}.5)$$

$$2\tilde{C}_{ab} = \frac{1}{2} \sum_{i=1}^{7} \sum_{c} \int dP_{cT} dX \tilde{\beta}_i(X, P_{cT}) \qquad (\bar{V}.6)$$

If ab is exotic the HF-conjecture gives $\tilde{C}_{ab} = 0$. Therefore from eq$(\bar{V}.6)$ either all $\tilde{\beta}_i(X, P_{cT}) \equiv 0$, or some $\tilde{\beta}_i(X, P_{cT})$ must have a negative sign according to the choice of X, P_{cT} and/or of c.

Thus a single particle inclusive cross-section may approach its limit from below. The criterion for such behaviour can be found within the above model.

From table-1- we see that for ab exotic only the $3^{\underline{rd}}$, $5^{\underline{th}}$, $6^{\underline{th}}$, and $7^{\underline{th}}$ components survive. The positivity of each component implies $\tilde{\beta}_i$ must be > 0 only if $\beta_i = 0$. Thus it is obvious that negative non-scaling pieces are only to be expected from the $5^{\underline{th}}$, $6^{\underline{th}}$, and the $7^{\underline{th}}$ components. The $7^{\underline{th}}$ component does not contribute to charge conservation. Thus we expect negative, non-scaling pieces from the $5^{\underline{th}}$ and $6^{\underline{th}}$ components.

From the above discussion we find that in the fragmentation region, if ab and $ab\bar{c}$ are exotic but $a\bar{c}$ and/or $b\bar{c}$ are not, then $f^{c,ab}$ will approach the scaling limit from below.

Continuing along the same line of reasoning ., Tye and Veneziano constructed table-4-, where each inclusive reaction has classified according to the exoticity of it is channels ab, $b\bar{c}$, $a\bar{c}$, and $ab\bar{c}$, and the properties of $f^{c,ab}$ in both fragmentation regions are given (see table -4-)

Table -4-

Channels exotic	Components present	Non-scaling part of $a+b \to c+x$) frag. of a $x>0$	frag. of b $x<0$	Examples ($ab \to cx$)	Remarks
none	all seven (plus 8 or 9)	+	+	$\pi^+N \to N$, π^+, π^0, K^+ $\pi^-N \to N$, π^-, π^0, K^0 $NN \to \pi$, K(?)	Components 8, 9 should be added when $a=c$ and or $b=c$. $\pi N \to N$ is expected to have positive non-scaling part because $\pi N \to$ meson approaches scaling from below.
ab	3, 5, 6, 7, (8, 9)	−	+	$NN \to N$, $KN \to K$, N(?)	
$b\bar{b}$	2, 4, 6, 7, (9)		+	$K^+N \to K^+$, K^0 $NN \to \bar{K}$	
$a\bar{c}$	1, 4, 5, 7, (8)	+		$\pi^+p \to \pi^+$, K $\pi^+n \to \pi^-$ $NN \to K$, $KN \to N$	
$ab\bar{c}$, ab	5, 6, 7	−	−	$KN \to \pi^0$, π^- $NN \to K$, π, Λ, K_1(?)	This is true independent of whether $f_2=0$ or not. Hence this provides a crucial test of the scaling.
$ab\bar{c}$, $b\bar{c}$	4, 6, 7		+	$\pi N \to N$, $\pi^-N \to K^-$ $\pi^0N \to K^0$	$f_2=0$ may change the positive signs here to negative for zero. This is particularly likely for reactions with components 5 plus 7 and 6 plus 7 only. It will be informative to measure $\sigma(K^-p \to \pi^-)$.
$ab\bar{c}$, $a\bar{c}$	4, 5, 7	+		$\pi^+p \to \pi^+$, K^0(?)	
$ab\bar{c}$, ab, $b\bar{c}$	6, 7	−	+	$\Lambda N \to K^-$	
$ab\bar{c}$, ab, $a\bar{c}$	5, 7	+	−	$KN \to \pi^+$	
$ab\bar{c}$, $a\bar{c}$, $b\bar{c}$	4, 7	+	+	$\pi^+N \to K^+$ $\pi^-N \to \bar{K}^0$	
all four	7	0	0	$NN \to N$, $\bar{K}$ $KN \to K$, N	This is assumed to be true.

Above we showed that only the components 3, 4, 5, and 6 of Fig.3.2 contribute to the non-scaling limit in the pionizat-ion region

From (III.4) we see that this scheme predicts that the rate at which the scaling limit should be approached is $s^{-1/4}$

In the above discussion the diffractive components have been neglected. It has been shown[20] that the presence of a large positive diffractive component (Fig.5.1) in the triple

Regge region in the form of Pomeron-Pomeron-Reggeon(PPR) will destroy the above scheme, since it may give rise to a negative $s^{-1/2}$ contribution to σ_{tot}, and thus eliminate the necessity for negative nonscaling pieces in components 5 and 6 (In the EGV scheme this component vanishes). At the moment there is no evidence for such a large component.

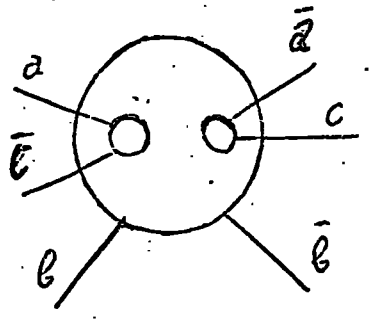

Fig.5.1

Above we said that this scheme predicts $s^{-1/4}$ rise in the pionization region. In Fig.5.2 we show an early analysis of the data by Ferbel et al, which concludes that an $s^{-1/4}$ behaviour does exist. But later more careful analysis by the Rutherford Group finds no sign of this $s^{-1/4}$ rise.

2) Another solution to the problem of the rising inclusive cross-section has beem suggested(see refernces (21) and (22))

There may be negative interference terms like those shown in Fig.5.3 . Or one of the particles a or b may diffractively dissociate into c,(Fig.5.1). Or for the rising in the central region[22] may have its origin in absorpative correction. In our opinion none of these suggestions gives a satisfactory solution to the problem, because they do not predict when negative non-scaling terms will occur (at this enegy dependence)

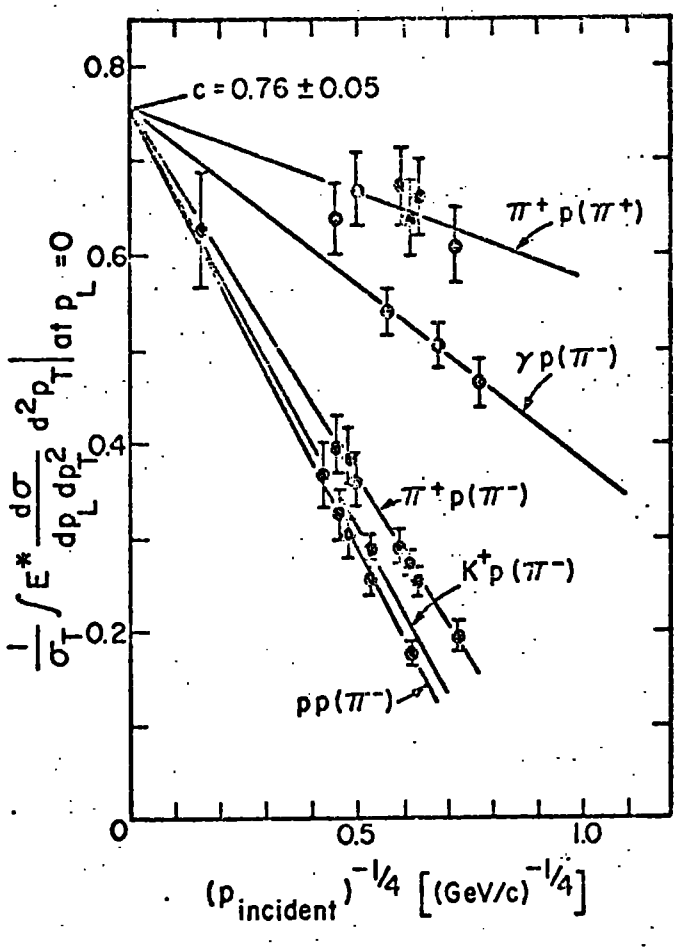
c = 0.76 ± 0.05
π⁺p(π⁺)
γp(π⁻)
π⁺p(π⁻)
K⁺p(π⁻)
pp(π⁻)
0.8
0.6
0.4
0.2
0
0.5
1.0
$\frac{1}{\sigma_T}\int E^* \frac{d\sigma}{dp_L\, dp_T^2}\, d^2p_T \Big|_{\text{at } p_L=0}$
$(p_{\text{incident}})^{-1/4}$ [(GeV/c)$^{-1/4}$]

Fig.5.2

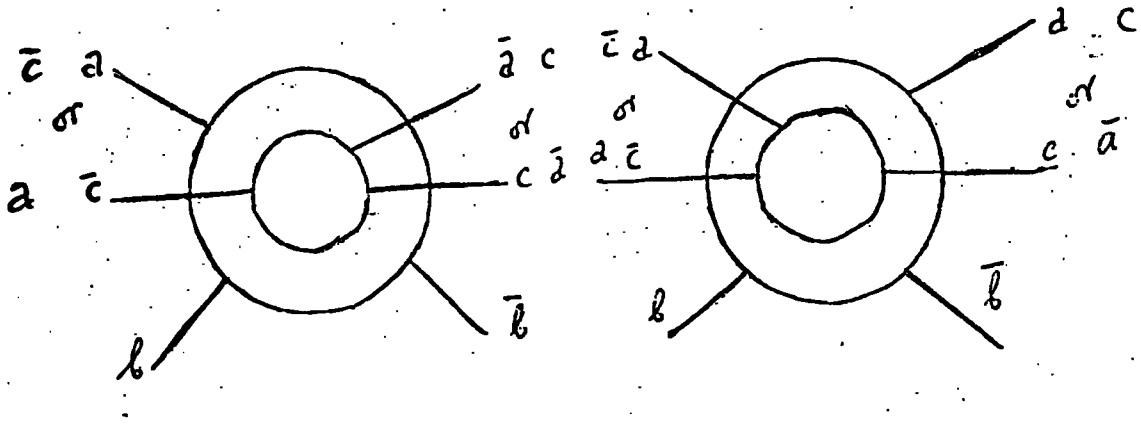
c̄ a
σ
a c̄
b
ā c
σ
c ā
b̄
c̄ a
σ
a c̄
b
ā c
σ
c ā
b̄

Fig.5.3

V.2. Conclusion.

To end this chapter we try to draw some conclusion about the various suggested criteria for scaling. In our opinion none of them is workable. In chapter IV we gave evidence for the failure of each criterion, though there are certainly some cases where they show some predictive power. But there is nothing surprising about this failure since even in the case of σ_{tot} we cannot apply the exoticity rules to the baryon-antibaryon interaction. Moreover, recent ISR data shows a logarithmic growth in the pp total cross-section, a reaction which has hitherto been regarded as good evidence for the duality scaling rules. In our opinion the problem with this sort of theory is more genral than simply the failure to predict correctly early scaling in one reaction or another. The main difficulty is really that the various criteria do not tell us at what energies one should expect scaling to occur, On the one hand we need high energies to achieve Regge dominance, but on the other hand the logarithmic behavior of cuts may alter the very high energy behavior.

Some people attempt to test scaling in terms of $f^{c,ab}/\sigma_{ab}$ but we cannot see any advantage in this. Indeed there is the disadvantage that if σ_{tot} itself scales then any scaling of the inclusive cross-section must be observed in $f^{c,ab}$ itself, but if σ_{tot} does not scale then there is no reason way $f^{c,ab}/\sigma_{tot}$ should scale.

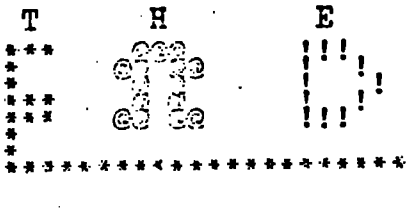

REFERENCES

1) C.Schmid — Proc. Roy. Soc. A. 318, 257 (1970).

2) P.D.B. Collins — Phys. Reports. 1C. No 4,105 (1971), Or see any book on high energy physics.

3) R.Dolen, D.Horn and C.Schmid — Phys. Rev. 166, 1768 (1968).

4) P.G.O.Freund — Phys. Rev. Letters 20, 235 (1968).

5) H.Harari — Phys. Rev. Letters 20, 1395 (1968).

6) K.Kikkawa, B.Sakita and M.A.Virasoro — Phys. Rev. 184, 1701 (1969).

K.Kikkawa, S.A.Klein B.Sakita, and M.A.Virasoro — Phys. Rev. D 1, 3258 (1970).

7) G.Veneziano — Nuovo Cimento 57A, 190 (1968).

8) A.DiGiacomo et al — Phys. Letters 33B, 171 (1970).

9) D.Gordon and G.V G.Veneziano — Phys. Rev. D 3, 2116 (1971).

10) S.H.H.Tye and G.Veneziano — Phys. Letters 38B, 30 (1972). Nuovo Cimento 14A, 711 (1973).

11) See reference 7

12) Look H.M.Chan — Rutherford Laboratory Preprint/T/21 (Regge Phenomenology of inclusive reactions.)

13) J.Benecke et al — Phys. Rev. 188, 2159 (1969)

14) R.P.Feynman Phys. Rev. Letters 23, 1415 (1969)

15) H.M.Chan,et al Phys. Rev. Letters 26, 672 (1971)

16) J.Ellis, et al Phys, Letters 25B, 227 (1971)

17) M.Einhorn et al Phys. Letters 37B, 292 (1971)
Phys. Rev D 6,1675 (1972)

18) See reference 10

19) See reference 10

20) See reference 10

21) See reference 17

22) Chan.H.M. et al Phys. Letters 40 B, 406 (1972)

Figure Captions

Fig.2.1 Transverse momentum distributions at X ≈ 0 observed atdifferent ISR energies, together with a typical distribution at accelerator energies.

Fig.2.2 Mean charged multiplicity in pp collisions at accelerator and ISR energies. The multiplicity is defined with respect to the inelastic cross-section. ($\langle n \rangle = (\sum_n n\sigma_n)/\sigma_{inl}$). The solid line gives a l logarithmic fit throug the accelerator data poits.

Fig.2.3 Longitudinal momentum distribution of protons and pions presented in terms of the Feynman variable X. The data points are ISR results at p_T=0.8 GeV/c. The solid lines run through data at accelerator energies.

Fig.4.1 Transvers momentum distrributions observed for differe different values of the scaling variable X, together with the corresponding distributions at accelerator energies.

Fig.4.2 Inclusive distribution of γ rays at very low trasverse momentum for different values of the scaling variable X, as the incident proton energy sweeps the 30-300 GeV range.

Fig.4.3 Inclusive distributions for π^-, observed at ISR energies and accelerator enegies.

Fig.4.4 The invariant π^- cross-section versus Y_{lab},

Fig.4.5 The rise of the π^- distribution at 90^o as observed by the Orsay-Strasbourg collaboration. One find a Rise by factor 2 between 20and 1000 GeV.

Fig.4.6 Same as Fig.4.4, for π^+.

Fig.4.7 Same as Fig.4.5, for π^+.

Fig.4.8 Inclusive distributions for Λ obtained in pp collisions between 6 and 200 GeV.

Fig.4.9 Inclusive $\pi^\pm$ distributions obtained in π^+p collisions at 8 and 16 GeV/c.

Fig.4.10 The inclusive cross-section for protons versus X.

Fig.4.11 Compilation of ISR results on $\bar{p}$ and p distributions obtained at different energies. The incident proton rapidity is kept fixed and an increasing rapidity interval is explored with increasing energy.

Fig.4.12 Same as Fig.4.10, for $\bar{p}$.

Fig.5.2 Inclusive π^- distributions at X = 0 for different reactions. The data are compared to an $s^{-1/4}$ approach to a scaling limit.